

Figure-eight solution in the complex time plane

Toshiaki Fujiwara

College of Liberal Arts and Sciences, Kitasato University

Note for a seminar at Kanazawa University on December 2, 2016
ver. December 11, 2016

The figure-eight solution is a periodic solution to the planar three-body problem under the homogeneous potential $1/r^\alpha$ with $\alpha > -2$ on which three bodies chase each other on one eight shaped orbit with a same time spacing,

$$(x_k(t), y_k(t)) = (x(t + kT/3), y(t + kT/3)), k = 0, 1, 2, \quad (1)$$

where T is the period. Since the potential with $\alpha = -2$ stands for free harmonic oscillators, no figure-eight solution exists.

The aim of this project is to understand analytic properties of figure eight solution in the complex time plane, $(x(z), y(z))$, $z \in \mathbb{C}$. Especially to understand the structure of singular points and the behavior of the solution around the points.

This note was prepared for the seminar at Kanazawa University on December 2, 2016. Some modifications and additions was made after the seminar.

Contents

1	Lagrangian and the equations of motion	2
1.1	Cartesian coordinates x_k and y_k	2
1.2	Complex variable $q_k = x_k + iy_k$ and $\tilde{q}_k = x_k - iy_k$	3
1.3	Variables for shape $\eta, \tilde{\eta}$, moment of inertia $I = r^2$ and rotation angle ψ	4
1.4	Shape sphere	6
1.5	Extension of the solution in $t \in \mathbb{R}$ to $z \in \mathbb{C}$	8
1.6	Comments	8
1.6.1	Degrees of freedom	8
1.6.2	A relation of q and \tilde{q} for “physical” solution	9
1.6.3	Comments for analytic continuation and periodicity $f(z) = f(z + 1)$	10
2	The figure-eight solution	12
2.1	Properties of periodic solutions	12
2.1.1	Properties of a periodic solution for $\alpha \neq 0, 2$	13
2.1.2	Properties of a periodic solution for $\alpha = 2$	13
2.1.3	Properties of a periodic solution for $\alpha = 0$	13
2.2	Properties of the figure-eight solution	13
2.2.1	Around an Euler configuration	14
2.2.2	Around an isosceles configuration	15

3	Numerical integrations by Mathematica	18
3.1	Integrations for complex variables on complex path	18
3.2	Method to take a proper branch in the equation of motion	18
3.3	Ask “NDSolve” to warm “an egg” with “other eggs”	18
4	Numerical calculations for $\alpha = 2$, a strong force potential	19
4.1	The initial conditions and the accuracy	19
4.2	Overview of the singularities	19
4.3	A “half collision”	21
4.4	Behavior of the shape variables	21
4.4.1	For the path $z = 0 \rightarrow 1/12$ (Euler config.) $\rightarrow 1/12 + i\tau$	22
4.4.2	For the path $z = 0 \rightarrow 1/12 \pm \epsilon \rightarrow 1/12 \pm \epsilon + i/10$	22
4.4.3	For the path $z = 0 \rightarrow k/6$ (isosceles) $\rightarrow k/6 + i\tau$	22
5	Numerical calculations for $\alpha = 0$, the log potential	25
5.1	Initial conditions and the accuracy	25
5.2	Overview of the singularities	26
5.3	Behavior of the variables	28
5.3.1	For the path $z = 0 \rightarrow k/6$ (isosceles config.) $\rightarrow k/6 + i\tau$	28
5.3.2	For the path $z = 0 \rightarrow 1/12$ (Euler config.) $\rightarrow 1/12 + 3i$	28
6	Series expansion around a “collision” point	31
6.1	A “full collision”, “half collision”, and simultaneous “half collision”	31
6.2	A series expansion around a possible simultaneous “half collision” for $\alpha = 2$	31
6.2.1	A simple solution	32

1 Lagrangian and the equations of motion

1.1 Cartesian coordinates x_k and y_k

Consider equal-mass planar three-body problem with $m_k = 1$, $k = 0, 1, 2$. Lagrangian L is defined by

$$L = \frac{1}{2} \sum_k \left(\left(\frac{dx_k}{dt} \right)^2 + \left(\frac{dy_k}{dt} \right)^2 \right) + U(x, y). \quad (2)$$

Here, the potential function $U(x, y)$ is given by for $\alpha \neq 0$,

$$U = \frac{1}{\alpha} \sum_{i,j} \frac{1}{\left((x_i - x_j)^2 + (y_i - y_j)^2 \right)^{\alpha/2}}, \quad (3)$$

and for $\alpha = 0$,

$$U = -\frac{1}{2} \sum_{i,j} \log \left((x_i - x_j)^2 + (y_i - y_j)^2 \right). \quad (4)$$

Then the equations of motion for all α , including $\alpha = 0$, are given by

$$\frac{d^2 x_k}{dt^2} = \sum_i \frac{x_i - x_k}{\left((x_i - x_j)^2 + (y_i - y_j)^2 \right)^{\alpha/2+1}} \text{ and } x \leftrightarrow y. \quad (5)$$

1.2 Complex variable $q_k = x_k + iy_k$ and $\tilde{q}_k = x_k - iy_k$

We can take alternative set of independent variables q_k, \tilde{q}_k defined by,

$$q_k(t) = x(t) + iy(t), \tilde{q}_k(t) = x(t) - iy(t) \Leftrightarrow x_k(t) = \frac{q_k + \tilde{q}_k}{2}, y_k(t) = \frac{q_k - \tilde{q}_k}{2i}. \quad (6)$$

Using

$$\begin{aligned} \left(\frac{dx_k}{dt}\right)^2 + \left(\frac{dy_k}{dt}\right)^2 &= \left(\frac{dx_k}{dt} + i\frac{dy_k}{dt}\right) \left(\frac{dx_k}{dt} - i\frac{dy_k}{dt}\right) \\ &= \frac{dq_k}{dt} \frac{d\tilde{q}_k}{dt}, \\ (x_i - x_j)^2 + (y_i - y_j)^2 &= \left((x_i - x_j) + i(y_i - y_j)\right) \left((x_i - x_j) - i(y_i - y_j)\right) \\ &= (q_i - q_j)(\tilde{q}_i - \tilde{q}_j), \end{aligned} \quad (7)$$

Lagrangian for $\alpha \neq 0$ is

$$L = \frac{1}{2} \frac{dq_k}{dt} \frac{d\tilde{q}_k}{dt} + \frac{1}{\alpha} \sum_{i,j} \frac{1}{\left((q_i - q_j)(\tilde{q}_i - \tilde{q}_j)\right)^{\alpha/2}},$$

and for $\alpha = 0$ is

$$L = \frac{1}{2} \frac{dq_k}{dt} \frac{d\tilde{q}_k}{dt} - \frac{1}{2} \sum_{i,j} \log \left((q_i - q_j)(\tilde{q}_i - \tilde{q}_j) \right).$$

However, if we use this Lagrangian, the canonical momentum p_k has factor 1/2, namely,

$$p_k = \frac{\partial L}{\partial \left(\frac{dq_k}{dt}\right)} = \frac{1}{2} \frac{d\tilde{q}_k}{dt}.$$

Although the factor 1/2 makes no problem, it is something awkward.

So, we use

$$\mathcal{L} = \frac{dq_k}{dt} \frac{d\tilde{q}_k}{dt} + \mathcal{U} \quad (8)$$

for Lagrangian. For $\alpha \neq 0$

$$\mathcal{U} = \frac{2}{\alpha} \sum_{i,j} \frac{1}{\left((q_i - q_j)(\tilde{q}_i - \tilde{q}_j)\right)^{\alpha/2}}, \quad (9)$$

and for $\alpha = 0$

$$\mathcal{U} = - \sum_{i,j} \log \left((q_i - q_j)(\tilde{q}_i - \tilde{q}_j) \right). \quad (10)$$

The momenta are, then, defined by

$$p_k = \frac{\partial \mathcal{L}}{\partial \left(\frac{dq_k}{dt}\right)} = \frac{d\tilde{q}_k}{dt}, \tilde{p}_i = \frac{dq_k}{dt}. \quad (11)$$

Note that canonical momentum p_k for q_k is not dq_k/dt but $d\tilde{q}_k/dt$. The Hamiltonian is given by

$$\mathcal{H} = \sum \left(p_k \frac{dq_k}{dt} + \tilde{p}_i \frac{d\tilde{q}_k}{dt} \right) - \mathcal{L} = \sum p_k \tilde{p}_i - \mathcal{U}. \quad (12)$$

This Hamiltonian is also twice of the usual one. The equations of motion for all α are given by

$$\begin{aligned} \frac{dq_k}{dt} &= \frac{\partial \mathcal{H}}{\partial p_k} = \tilde{p}_k, & \frac{d\tilde{p}_k}{dt} &= -\frac{\partial \mathcal{H}}{\partial \tilde{q}_k} = \sum_j \frac{q_j - q_k}{\left((q_j - q_k)(\tilde{q}_j - \tilde{q}_k) \right)^{\alpha/2+1}}, \\ \frac{d\tilde{q}_k}{dt} &= \frac{\partial \mathcal{H}}{\partial \tilde{p}_k} = p_k, & \frac{dp_k}{dt} &= -\frac{\partial \mathcal{H}}{\partial q_k} = \sum_j \frac{\tilde{q}_j - \tilde{q}_k}{\left((q_j - q_k)(\tilde{q}_j - \tilde{q}_k) \right)^{\alpha/2+1}}. \end{aligned} \quad (13)$$

1.3 Variables for shape $\eta, \tilde{\eta}$, moment of inertia $I = r^2$ and rotation angle ψ

To describe the motion of the shape of the triangle $q_0 q_1 q_2$, let us introduce the shape variable η and $\tilde{\eta}$ defined by

$$\eta = \frac{\sqrt{3} q_0}{q_2 - q_1}, \quad \tilde{\eta} = \frac{\sqrt{3} \tilde{q}_0}{\tilde{q}_2 - \tilde{q}_1}. \quad (14)$$

We also use η_x and η_y defined by

$$\eta_x = \frac{\eta + \tilde{\eta}}{2}, \quad \eta_y = \frac{\eta - \tilde{\eta}}{2i} \Leftrightarrow \eta = \eta_x + i\eta_y, \quad \tilde{\eta} = \eta_x - i\eta_y. \quad (15)$$

The explicit expression for η_x and η_y by x_k and y_k are

$$\begin{aligned} \eta_x &= \frac{\sqrt{3} \left(x_0(x_2 - x_1) + y_0(y_2 - y_1) \right)}{(x_2 - x_1)^2 + (y_2 - y_1)^2}, \\ \eta_y &= \frac{\sqrt{3} \left(y_0(x_2 - x_1) - x_0(y_2 - y_1) \right)}{(x_2 - x_1)^2 + (y_2 - y_1)^2}. \end{aligned} \quad (16)$$

The geometrical description of these variables are in the following. Using a similarity transformation and translation, map $q_1 \rightarrow -1/\sqrt{3}$ and $q_2 \rightarrow +1/\sqrt{3}$, then q_0 is mapped to η . See figure 1. The explicit form for this map is

$$z \rightarrow \frac{2}{\sqrt{3}} \left(\frac{z - q_1}{q_2 - q_1} - \frac{1}{2} \right). \quad (17)$$

One can easily check

$$q_1 \rightarrow -\frac{1}{\sqrt{3}}, \quad q_2 \rightarrow +\frac{1}{\sqrt{3}}, \quad \text{and} \quad q_0 \rightarrow \eta = \frac{\sqrt{3} q_0}{q_2 - q_1}, \quad (18)$$

using $q_0 + q_1 + q_2 = 0$. In this variable two body collisions are expressed by $\eta = \pm 1/\sqrt{3}$ and ∞ . Actually, for collision the bodies 0 and 1 at $q_0 = q_1 = Q$, we have $q_2 = -2Q$ and $\eta = \sqrt{3}Q/(-2Q - Q) = -1/\sqrt{3}$. Similarly, $\eta = +1/\sqrt{3}$ for collision 0 and 2 and $\eta = \infty$ for collision 1 and 2.

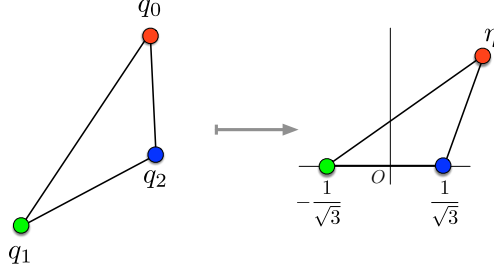


Figure 1: Triangle $q_0q_1q_2$ and the definition of the shape variable η .

To recover the variables q_k and \tilde{q}_k from η and $\tilde{\eta}$, we have to recover size variable r and angle variable ψ as follows. Let us define the variable ξ_k whose center of mass is fixed at the origin subtracting the center of mass $\eta/3$ from the triangle $-1/\sqrt{3}$, $+1/\sqrt{3}$, and η ,

$$\xi_0 = \eta - \frac{\eta}{3} = \frac{2\eta}{3}, \quad \xi_1 = -\frac{1}{\sqrt{3}} - \frac{\eta}{3}, \quad \xi_2 = \frac{1}{\sqrt{3}} - \frac{\eta}{3}, \quad (19)$$

and replace η to $\tilde{\eta}$ to get $\tilde{\xi}_k$. Since the triangle $\xi_0\xi_1\xi_2$ is similar to the triangle $q_0q_1q_2$, there exist $r, \psi \in \mathbb{R}$ that satisfy

$$q_k = r e^{i\psi} \frac{\xi_k}{\sqrt{\sum \xi_k \tilde{\xi}_k}}, \quad \tilde{q}_k = r e^{-i\psi} \frac{\tilde{\xi}_k}{\sqrt{\sum \xi_k \tilde{\xi}_k}}. \quad (20)$$

Here, r^2 turns out to be the moment of inertia,

$$I = \sum (x_k^2 + y_k^2) = \sum q_k \tilde{q}_k = r^2. \quad (21)$$

Substituting (20) into (8), we get the Lagrangian for $r, \psi, \eta, \tilde{\eta}$,

$$\mathcal{L} = \left(\frac{dr}{dt} \right)^2 + r^2 \left(\frac{d\psi}{dt} + \frac{1}{2i(1+\eta\tilde{\eta})} \left(\tilde{\eta} \frac{d\eta}{dt} - \eta \frac{d\tilde{\eta}}{dt} \right) \right)^2 + r^2 \frac{1}{(1+\eta\tilde{\eta})^2} \frac{d\eta}{dt} \frac{d\tilde{\eta}}{dt} + \mathcal{U}(r, \eta, \tilde{\eta}). \quad (22)$$

Potential for $\alpha \neq 0$ is

$$\mathcal{U} = \frac{2}{\alpha r^\alpha} \left(\frac{1+\eta\tilde{\eta}}{2} \right)^{\alpha/2} \left(1 + \frac{2^\alpha}{\left((1-\sqrt{3}\eta)(1-\sqrt{3}\tilde{\eta}) \right)^{\alpha/2}} + \frac{2^\alpha}{\left((1+\sqrt{3}\eta)(1+\sqrt{3}\tilde{\eta}) \right)^{\alpha/2}} \right), \quad (23)$$

and for $\alpha = 0$ is

$$\mathcal{U} = -6 \log r + 3 \log(1+\eta\tilde{\eta}) - \log(1-3\eta^2)(1-3\tilde{\eta}^2) + \log 2. \quad (24)$$

Sometimes, it is useful to use μ_k defined by

$$\mu_0 = \frac{1+\eta\tilde{\eta}}{2}, \quad \mu_1 = \frac{2(1+\eta\tilde{\eta})}{(1-\sqrt{3}\eta)(1-\sqrt{3}\tilde{\eta})}, \quad \mu_2 = \frac{2(1+\eta\tilde{\eta})}{(1+\sqrt{3}\eta)(1+\sqrt{3}\tilde{\eta})}. \quad (25)$$

There is an identity

$$\frac{1}{\mu_0} + \frac{1}{\mu_1} + \frac{1}{\mu_2} = 3. \quad (26)$$

The expression for potentials are for $\alpha \neq 0$

$$\mathcal{U} = \frac{2}{\alpha r^\alpha} \left(\mu_0^{\alpha/2} + \mu_1^{\alpha/2} + \mu_2^{\alpha/2} \right), \quad (27)$$

and for $\alpha = 0$

$$\mathcal{U} = -6 \log r + \log(\mu_0 \mu_1 \mu_2). \quad (28)$$

The Lagrangian does not depend on ψ , the angular momentum p_ψ is constant and zero for the figure-eight solution,

$$p_\psi = \frac{\partial \mathcal{L}}{\partial \left(\frac{d\psi}{dt} \right)} = 2r^2 \left(\frac{d\psi}{dt} + \frac{1}{2i(1 + \eta\tilde{\eta})} \left(\tilde{\eta} \frac{d\eta}{dt} - \eta \frac{d\tilde{\eta}}{dt} \right) \right) = 0. \quad (29)$$

Therefore, the equation for ψ is,

$$\frac{d\psi}{dt} = -\frac{1}{2i(1 + \eta\tilde{\eta})} \left(\tilde{\eta} \frac{d\eta}{dt} - \eta \frac{d\tilde{\eta}}{dt} \right). \quad (30)$$

Integrating this equation, we get the expression for the rotation angle

$$\psi(t) = -\int_0^t \frac{1}{2i(1 + \eta\tilde{\eta})} \left(\tilde{\eta} \frac{d\eta}{dt} - \eta \frac{d\tilde{\eta}}{dt} \right) dt + \psi(0). \quad (31)$$

The other momenta are

$$\begin{aligned} p_r &= 2 \frac{dr}{dt}, \\ p_\eta &= \frac{r^2}{(1 + \eta\tilde{\eta})^2} \frac{d\tilde{\eta}}{dt}, \quad p_{\tilde{\eta}} = \frac{r^2}{(1 + \eta\tilde{\eta})^2} \frac{d\eta}{dt}. \end{aligned} \quad (32)$$

The Hamiltonian \mathcal{H} is

$$\mathcal{H} = \frac{p_r^2}{4} + \frac{(1 + \eta\tilde{\eta})^2}{r^2} p_\eta p_{\tilde{\eta}} - \mathcal{U}. \quad (33)$$

Here, we have dropped the term that proportional to the angular momentum $p_\psi = 0$.

1.4 Shape sphere

The kinetic energy for the shape variable defines the metric

$$\frac{d\eta d\tilde{\eta}}{(1 + \eta\tilde{\eta})^2} = \frac{d\eta_x^2 + d\eta_y^2}{(1 + \eta_x^2 + \eta_y^2)^2} \quad (34)$$

of the Riemann sphere whose radius is $1/2$. Actually, the coordinates

$$X = \frac{\eta_x}{1 + \eta_x^2 + \eta_y^2}, \quad Y = \frac{\eta_y}{1 + \eta_x^2 + \eta_y^2}, \quad \text{and} \quad Z = 1 - \frac{1}{1 + \eta_x^2 + \eta_y^2} \quad (35)$$

satisfy

$$X^2 + Y^2 + \left(Z - \frac{1}{2} \right)^2 = \frac{1}{4} \quad (36)$$

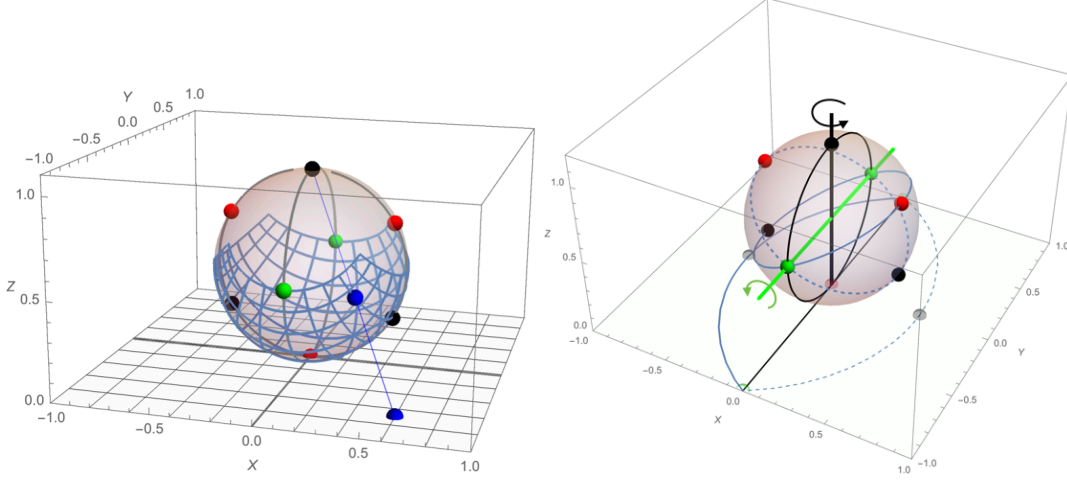


Figure 2: The shape plane and the shape sphere. The black, red, green points correspond to collisions, Euler configurations, and Lagrange configurations. Left: Projection of a point on the shape plane to the shape sphere. Right: Cyclic exchange of indexes of q_k $0 \rightarrow 1 \rightarrow 2 \rightarrow 0$ corresponds to $2\pi/3$ rotation around the axis (green line) that connect two Lagrange points. Exchange of $1 \leftrightarrow 2$ corresponds to π rotation around the axis (black line) that connects a Euler point and a two body collision.

and

$$dX^2 + dY^2 + dZ^2 = \frac{d\eta_x^2 + d\eta_y^2}{(1 + \eta_x^2 + \eta_y^2)^2}. \quad (37)$$

The Euler points $(\eta_x, \eta_y) = (0, 0), (\pm\sqrt{3})$ are mapped to $(X, Y, Z) = (0, 0, 0), (\pm\sqrt{3}/4, 0, 3/4)$. The Lagrange points $(\eta_x, \eta_y) = (0, \pm 1)$ are mapped to $(X, Y, Z) = (0, \pm 1/2, 1/2)$.

Let us use a polar coordinates whose Z' axes is the line connection two Lagrange points, $Z' = -Y = \sin(\theta)/2$, $X' = 1/2 - Z = \cos(\theta) \cos(\phi)/2$, $Y' = \cos(\theta) \sin(\phi)/2$. Namely,

$$\begin{aligned} X &= \frac{\eta_x}{1 + \eta_x^2 + \eta_y^2} = \frac{1}{2} \cos \theta \sin \phi, \\ Y &= \frac{\eta_y}{1 + \eta_x^2 + \eta_y^2} = -\frac{1}{2} \sin \theta, \\ Z &= 1 - \frac{1}{1 + \eta_x^2 + \eta_y^2} = \frac{1}{2} - \frac{1}{2} \cos \theta \cos \phi. \end{aligned} \quad (38)$$

Inversely,

$$1 + \eta_x^2 + \eta_y^2 = \frac{2}{1 + \cos \theta \cos \phi}, \quad (39)$$

$$\text{and } (\eta_x, \eta_y) = \frac{(\cos \theta \sin \phi, -\sin \theta)}{1 + \cos \theta \cos \phi}. \quad (40)$$

Then, we have

$$\frac{d\eta_x^2 + d\eta_y^2}{(1 + \eta_x^2 + \eta_y^2)^2} = \frac{1}{4} (d\theta^2 + (\cos \theta)^2 d\phi^2) \quad (41)$$

and

$$\frac{\eta_x d\eta_y - \eta_y d\eta_x}{1 + \eta_x^2 + \eta_y^2} = \frac{-\sin \phi d\theta + \cos \theta \sin \theta \cos \phi d\phi}{2(1 + \cos \theta \cos \phi)}. \quad (42)$$

The expression for the three functions μ_k by θ and ϕ are,

$$\mu_0 = \frac{1}{1 + \cos \theta \cos \phi}, \quad \mu_1 = \frac{1}{1 + \cos \theta \cos(\phi + 2\pi/3)}, \quad \mu_2 = \frac{1}{1 + \cos \theta \cos(\phi - 2\pi/3)}. \quad (43)$$

Then, the Lagrangian for r, θ, ϕ is

$$\mathcal{L} = \left(\frac{dr}{dt}\right)^2 + \frac{r^2}{4} \left(\left(\frac{d\theta}{dt}\right)^2 + (\cos \theta)^2 \left(\frac{d\phi}{dt}\right)^2 \right) + \mathcal{U}. \quad (44)$$

Here, the term proportional to the angular momentum p_ψ^2 is dropped.

Symmetric polynomials of μ_k can be expressed by θ and 3ϕ ,

$$\mu_0 + \mu_1 + \mu_2 = \frac{3(7 - \cos(2\theta))}{2(\cos \theta)^3 \cos(3\phi) - 6(\cos \theta)^2 + 8}, \quad (45)$$

$$\mu_0 \mu_1 \mu_2 = \frac{16}{10 - 6 \cos(2\theta) + (3 \cos \theta + \cos(3\theta)) \cos(3\phi)}, \quad (46)$$

and $\mu_0 \mu_1 + \mu_1 \mu_2 + \mu_2 \mu_0 = 3\mu_0 \mu_1 \mu_2$ by the identity (26).

The cyclic permutation of the indexes $0 \rightarrow 1 \rightarrow 2 \rightarrow 0$ makes a transform of $\eta \rightarrow \eta'$

$$\eta = \frac{\sqrt{3}q_0}{q_2 - q_1} \rightarrow \eta' = \frac{\sqrt{3}q_1}{q_0 - q_2} = \frac{\sqrt{3} + \eta}{1 - \sqrt{3}\eta} \quad (47)$$

that is equivalent to the rotation in the shape sphere $\phi \rightarrow \phi + 2\pi/3$. On the other hand, the exchange of indexes $1 \leftrightarrow 2$ makes the rotation $\eta \rightarrow \eta' = -\eta$ that is equivalent to $\theta \rightarrow -\theta$ and $\phi \rightarrow -\phi$. See figure 2.

1.5 Extension of the solution in $t \in \mathbb{R}$ to $z \in \mathbb{C}$

We extend the time $t \in \mathbb{R}$ to $z \in \mathbb{C}$.

$$\begin{aligned} \frac{dq_k}{dz} &= \frac{\partial \mathcal{H}}{\partial p_k}, & \frac{d\tilde{p}_i}{dz} &= -\frac{\partial \mathcal{H}}{\partial \tilde{q}_k}, \\ \frac{d\tilde{q}_k}{dz} &= \frac{\partial \mathcal{H}}{\partial \tilde{p}_i}, & \frac{dp_k}{dz} &= -\frac{\partial \mathcal{H}}{\partial q_k}. \end{aligned} \quad (48)$$

Integrating this equations with the initial condition for the figure-eight solution at $z = 0$, we get the analytic continuation of $q_k(z), \tilde{q}_k(z), p_k(z), \tilde{p}_i(z)$.

1.6 Comments

1.6.1 Degrees of freedom

Originally, we have 6 independent variables x_k and y_k . Then we take their linear combination $q_k = x_k + iy_k$ and $\tilde{q} = x_k - iy_k$, again we have 6 independent variables. Taking the center of mass frame $\sum x_k = \sum y_k = 0$, we have 4 independent variables. Similarly, $\sum q_k = \sum \tilde{q}_k = 0$ leave us

4 independent variables. Then, we use $\{r, \psi, \eta, \tilde{\eta}\}$ or $\{r, \psi, \eta_x, \eta_y\}$, again we have 4 independent variables. In summary,

$$\begin{cases} x_k, y_k, k = 0, 1, 2 \\ \sum x_k = \sum y_k = 0 \end{cases} \Leftrightarrow \begin{cases} q_k, \tilde{q}_k, k = 0, 1, 2 \\ \sum q_k = \sum \tilde{q}_k = 0 \end{cases} \Leftrightarrow r, \psi, \eta, \tilde{\eta}. \quad (49)$$

And three sets for shape variables

$$\eta, \tilde{\eta} \Leftrightarrow \eta_x, \eta_y \Leftrightarrow \theta, \phi. \quad (50)$$

The relations used to convert the variables are just algebraic equations that hold for any number whether the number are real or complex.

The variables q_k and \tilde{q}_k are independent variable, as well as x_k and y_k are independent. We can see that the equations of motion (13) are equivalent to the equations (5). Let us see the Euler-Lagrange equations for the Lagrangian \mathcal{L} , closely. The partial derivative of \mathcal{U} by q_k for $\alpha \neq 0$, treating q and \tilde{q} are independent variable, is

$$\frac{\partial \mathcal{U}}{\partial q_k} = - \sum_j \frac{1}{(q_k - q_j)^{\alpha/2+1} (\tilde{q}_k - \tilde{q}_j)^{\alpha/2}} = - \sum_j \frac{\tilde{q}_k - \tilde{q}_j}{((q_k - q_j)(\tilde{q}_k - \tilde{q}_j))^{\alpha/2+1}}, \quad (51)$$

and for $\alpha = 0$ is

$$\frac{\partial \mathcal{U}}{\partial q_k} = - \sum_j \frac{1}{(q_k - q_j)} = - \sum_j \frac{\tilde{q}_k - \tilde{q}_j}{(q_k - q_j)(\tilde{q}_k - \tilde{q}_j)}. \quad (52)$$

Therefore, for all α including $\alpha = 0$,

$$\frac{\partial \mathcal{U}}{\partial q_k} = - \sum_j \frac{\tilde{q}_k - \tilde{q}_j}{((q_k - q_j)(\tilde{q}_k - \tilde{q}_j))^{\alpha/2+1}}, \quad (53)$$

On the other hand, the partial derivative \mathcal{L} by dq_k/dt , treating dq_k/dt and $d\tilde{q}_k/dt$ are independent variables, is

$$\frac{\partial \mathcal{L}}{\partial \left(\frac{dq_k}{dt} \right)} = \frac{\partial}{\partial \left(\frac{dq_k}{dt} \right)} \left(\frac{dq_k}{dt} \frac{d\tilde{q}_k}{dt} \right) = \frac{d\tilde{q}_k}{dt}. \quad (54)$$

Therefore, the Euler-Lagrange equations by q_k yield

$$\frac{d}{dt} \frac{\partial \mathcal{L}}{\partial \left(\frac{dq_k}{dt} \right)} = \frac{\partial \mathcal{U}}{\partial q_k} \Rightarrow \frac{d^2 \tilde{q}_k}{dt^2} = - \sum_j \frac{\tilde{q}_k - \tilde{q}_j}{((q_k - q_j)(\tilde{q}_k - \tilde{q}_j))^{\alpha/2+1}}. \quad (55)$$

Similar calculations by \tilde{q}_k yield

$$\frac{d^2 q_k}{dt^2} = - \sum_j \frac{q_k - q_j}{((q_k - q_j)(q_k - q_j))^{\alpha/2+1}}. \quad (56)$$

The equations (55) and (56) are equivalent to the equations of motion for x_k and y_k in (5).

1.6.2 A relation of q and \tilde{q} for “physical” solution

We call a solution “physical” when the value of the solution is real for real time,

$$\{x(t), y(t)\} : \text{“physical”} \Leftrightarrow x(t), y(t) \in \mathbb{R} \text{ for } t \in \mathbb{R}. \quad (57)$$

Therefore, for “physical” solution, $q(t) = x(t) + iy(t)$ and $\tilde{q}(t) = x(t) - iy(t)$ in $t \in \mathbb{R}$ are mutually complex conjugate.

Analytic continuation of the “physical” solution, however, makes $x(z), y(z)$ complex for $z \in \mathbb{C}$. Therefore, $q(z) = x(z) + iy(z)$ and $\tilde{q}(z) = x(z) - iy(z)$ are no longer complex conjugate of each other. Are there any relation between q and \tilde{q} ? Yes. To see this relation, remember a fact of analytic function.

In general, for a function $f(z)$ which is analytic in a region \mathbb{D} that contains a real interval, $(f(z^*))^*$ (* represents complex conjugate) is also an analytic function of z , because the following limit

$$\lim_{h \rightarrow 0} \frac{(f(z^* + h^*))^* - (f(z^*))^*}{h} = \lim_{h \rightarrow 0} \left(\frac{f(z^* + h^*) - f(z^*)}{h^*} \right)^* \quad (58)$$

yields a fixed value for any direction of $h \rightarrow 0$. We write this function $f^\dagger(z)$. For a series expansion $f(z) = \sum a_n z^n$, $f^\dagger(z)$ is given by $f^\dagger(z) = \sum a_n^* z^n$. For example, $\sin^\dagger(z) = \sin(z)$, $\cos^\dagger(z) = \cos(z)$, and for $f(z) = e^{iz}$, $f^\dagger(z) = e^{-iz}$. Sometimes $f^\dagger(z)$ is called a “mirror image” of $f(z)$. The correspondence between $f(z)$ and $f^\dagger(z)$ is one to one. All information for $f^\dagger(z)$ is contained in $f(z)$.

If $f(z)$ is analytic in \mathbb{D} and $f(t) \in \mathbb{R}$ for $t \in \mathbb{R}$, then $f^\dagger(z) = f(z)$ in \mathbb{D} . This is because $f^\dagger(t) = (f(t^*))^* = f(t)$ for $t \in \mathbb{R}$, and analytic continuation keeps this relation for $t \in \mathbb{C}$. If this function is even, $f(-z) = f(z)$, then $f(i\tau)$ is real, and if odd then it is pure imaginary for $\tau \in \mathbb{R}$. This is obvious by the series expansion of $f(z)$ at $z = 0$. Another proof of this property is given by the relation $f(z) = f^\dagger(z) = (f(z^*))^*$. Namely, $f(z)^* = f(z^*)$. Then, $f(i\tau)^* = f(-i\tau) = \pm f(i\tau)$.

Now, let us back to the relation of q and \tilde{q} . For “physical” solutions, including the figure-eight solution, both $x(z)$ and $y(z)$ are analytic around the real axis $z = t \in \mathbb{R}$ and have real value on the real axis. Therefore,

$$\text{for “physical” solution, } x^\dagger(z) = x(z) \text{ and } y^\dagger(z) = y(z). \quad (59)$$

Then,

$$\text{for “physical” solution, } \tilde{q}(z) = q^\dagger(z) = (q(z^*))^* \text{ and } q(z) = \tilde{q}^\dagger(z) = (\tilde{q}(z^*))^* \text{ for } z \in \mathcal{D}. \quad (60)$$

Thus, for physical solution, $\tilde{q}(z)$ is a “mirror image” of q and all information for $\tilde{q}(z)$ is contained in $q(z)$. See figure 3. Similarly, $\eta_x^\dagger(z) = \eta_x$, $\eta_y^\dagger(z) = \eta_y$ (See the equation (16)), $r^\dagger(z) = r(z)$ and $\psi^\dagger(z) = \psi(z)$, therefore $\eta^\dagger = \tilde{\eta}$ and $\tilde{\eta}^\dagger = \eta$, for “physical” solution.

Note that even for “physical” solution, $q(z_0) = x(z_0) + iy(z_0) = 0$ for $z_0 \notin \mathbb{R}$ does NOT always imply $\tilde{q}(z_0) = x(z_0) - iy(z_0) = 0$, although $q(t) = x(t) + iy(t) = 0$ in $t \in \mathbb{R}$ always imply $\tilde{q}(t) = x(t) - iy(t) = 0$. In general,

$$\text{for “physical” solution, } q(z_0) = 0 \Leftrightarrow \tilde{q}(z_0^*) = 0. \quad (61)$$

Because, $\tilde{q}(z_0^*) = q^\dagger(z_0^*) = (q(z_0))^* = 0$. For example, $x(t) = 5t$ and $y(t) = 5t^2$ is a “physical” solution for $d^2x/dt^2 = 0$ and $d^2y/dt^2 = 10$, the free fall problem. Then $q(z) = 5(z + iz^2)$ and $\tilde{q}(z) = 5(z - iz^2)$ surely satisfy $q^\dagger(z) = \tilde{q}(z)$ and $\tilde{q}^\dagger(z) = q(z)$ and $q(i) = 5(i - i) = 0$ while $\tilde{q}(i) = 5(i + i) = 10i \neq 0$. Surely, $\tilde{q}(-i) = 5(-i + i) = 0$ is satisfied.

1.6.3 Comments for analytic continuation and periodicity $f(z) = f(z + 1)$

Let functions $f(t)$ and $g(t)$ be equal on the real axis, and both are analytic for a region that contains the real axis. Then $h(z) = f(z) - g(z) = 0$ for the region, and analytic continuation of the function $h(z) = 0$ yields $h(z) = 0$ for all $z \in \mathbb{C}$. Therefore,

$$f(t) = g(t) \text{ on } t \in \mathbb{R} \Rightarrow f(z) = g(z) \text{ for all } z \in \mathbb{C}.$$

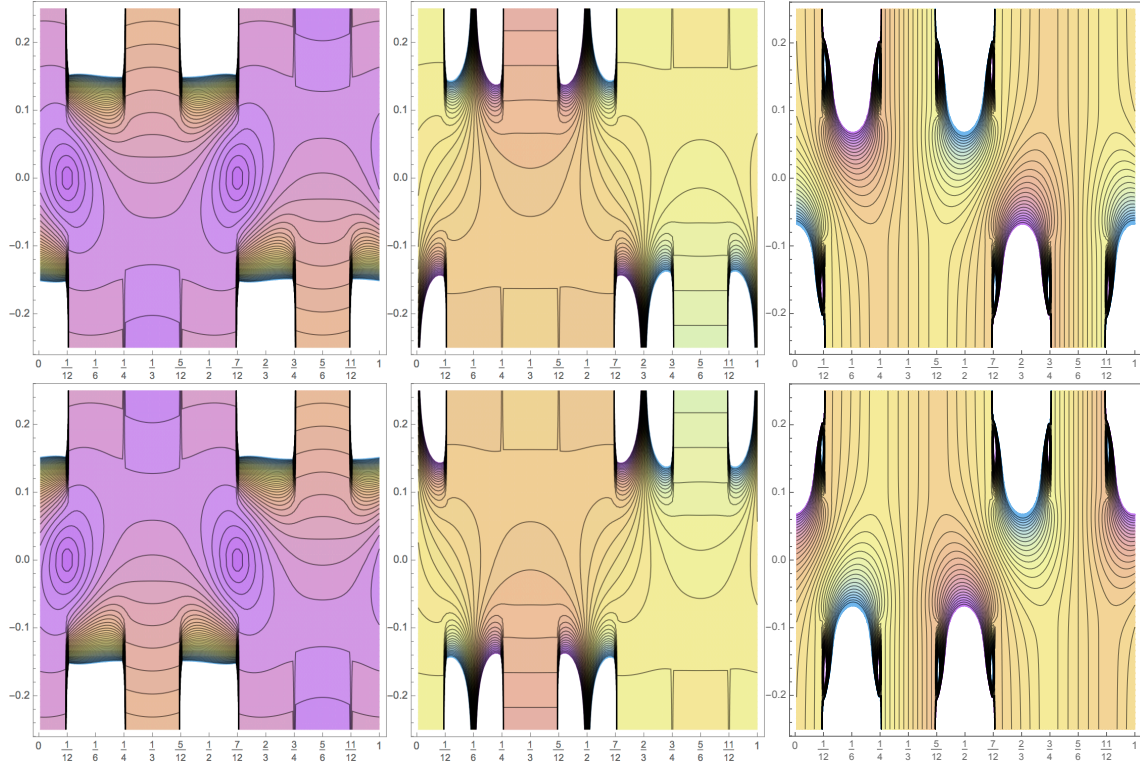


Figure 3: For “physical” solution, $q(z)$ and $\tilde{q}(z)$ are “mirror image” of each other, namely, $\tilde{q}(z) = (q(z^*))^*$. Figures for $q(z)$ and $\tilde{q}(z)$ for figure-eight solution for $\alpha = 2$ with period $T = 1$ are shown. The upper row from left to right: $|q(z)|$, $\Re(q(z))$, and $\Im(q(z))$. The lower row from left to right: $|\tilde{q}(z)|$, $\Re(\tilde{q}(z))$, and $\Im(\tilde{q}(z))$. The region $z = t + i\tau$, $t \in [0, 1]$, $\tau \in [-0.25, 0.25]$ is shown. The white region shows areas where values are too positively large or negatively large.

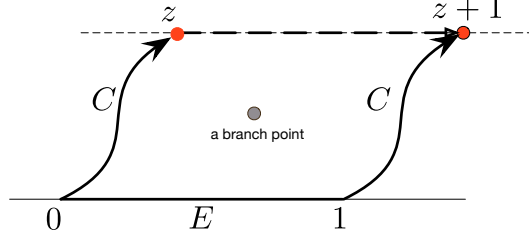


Figure 4: The function $f(t)$ has period 1 on the real axis (the solid line). Then, $f(C; z) = f(EC; z + 1)$ (the thick solid lines), while $f(C; z) \neq f(CE; z + 1)$ (the dashed line) if the closed path $C^{-1}ECE^{-1}$ encloses a branch point. Therefore, $f(z)$ has no period along the dashed line, in general.

Be careful. This may be correct in some sense, and at the same time be incorrect in other sense, because both of the function can be multivalued. In one branch $f(z) = g(z)$ may holds, while in other branch $f(z) \neq g(z)$.

For multivalued function, let us specify the path on what we integrated from the origin to z . We write the function f whose initial point is 0 and integrated on the path C be $f(C; z)$. If we first integrated on C_1 and then on C_2 to reach z , we write $f(C_1C_2; z)$. So, the above equation should be

$$f(t) = g(t) \text{ on } t \in \mathbb{R} \Rightarrow f(C; z) = g(C; z) \text{ for all } z \in \mathbb{C} \text{ and all path } C. \quad (62)$$

For example, let f be a function with period 1, $f(t) = f(t + 1)$ on the real axis. In our notation, $f(E^t; t) = f(EE^t; t + 1)$, where path E^t and E represent the path on the real axis with length t and unit length. Then

$$f(t) = f(t + 1) \text{ on } t \in \mathbb{R} \Rightarrow f(C; z) = f(EC; z + 1) \text{ for all } z \in \mathbb{C} \text{ and all path } C. \quad (63)$$

If the path $C^{-1}ECE^{-1}$ encloses a branch point, $f(C; z) \neq f(CE; z + 1)$. See figure 4.

2 The figure-eight solution

2.1 Properties of periodic solutions

The second derivative of the moment of inertia is

$$\begin{aligned} \frac{d^2 I}{dt^2} &= 2 \frac{d}{dt} \sum \left(x_k \frac{dx_k}{dt} + y_k \frac{dy_k}{dt} \right) \\ &= 2 \sum \left(\left(\frac{dx_k}{dt} \right)^2 + \left(\frac{dy_k}{dt} \right)^2 \right) + 2 \sum \left(x_k \frac{\partial}{\partial x_k} + y_k \frac{\partial}{\partial y_k} \right) U. \end{aligned} \quad (64)$$

For $\alpha \neq 0$, the second term yields $-2\alpha U$. Therefore,

$$\frac{d^2 I}{dt^2} = 2 \sum \left(\left(\frac{dx_k}{dt} \right)^2 + \left(\frac{dy_k}{dt} \right)^2 \right) - 2\alpha U = 4E + (4 - 2\alpha)U. \quad (65)$$

On the other hand, for $\alpha = 0$, $\sum (x_k \partial / \partial x_k + y_k \partial / \partial y_k) U = -3$. Therefore

$$\frac{d^2 I}{dt^2} = 2 \sum \left(\left(\frac{dx_k}{dt} \right)^2 + \left(\frac{dy_k}{dt} \right)^2 \right) - 6. \quad (66)$$

2.1.1 Properties of a periodic solution for $\alpha \neq 0, 2$

Integrating the relation (65) for one period, we get the virial theorem,

$$J = \int_0^T dt \sum \left(\left(\frac{dx_k}{dt} \right)^2 + \left(\frac{dy_k}{dt} \right)^2 \right) = \alpha \int_0^T dt U. \quad (67)$$

The left hand side is the action variable or the abbreviated action J defined by

$$J = \oint \sum \left(\frac{dx_k}{dt} dx_k + \frac{dy_k}{dt} dy_k \right). \quad (68)$$

Integration of $E = 1/2 \sum ((dx_k/dt)^2 + (dy_k/dt)^2) - U$ for one period yields $ET = J/2 - \int dt U = J/2 - J/\alpha$. Here, we have used the relation (67). Therefore, for $\alpha \neq 0, 2$,

$$J = \frac{2\alpha}{\alpha - 2} ET. \quad (69)$$

Substituting $T = dJ/dE$, we get $J = 2\alpha/(\alpha - 2) \times EdJ/dE$. Integration of this relation yields,

$$J = D|E|^{(\alpha-2)/(2\alpha)}, \quad (70)$$

where D is a constant and scale invariant.

2.1.2 Properties of a periodic solution for $\alpha = 2$

The case $\alpha = 2$ is special. In this case $d^2I/dt^2 = 4E$. Integration this relation yields $I = 2Et^2 + c_1t + c_0$, where c_1 and c_0 are constant. Therefore, for any periodic solution in $\alpha = 2$,

$$E = 0 \text{ and } I = c_0. \quad (71)$$

The action variable $J = D$ is scale invariant.

2.1.3 Properties of a periodic solution for $\alpha = 0$

Since $\sum (x_k \partial / \partial x_k + y_k \partial / \partial y_k) U = -3$ for $\alpha = 0$, the action variable is simply

$$J = 3T. \quad (72)$$

Therefore, $J = 3dJ/dE$ yields

$$J = De^{|E|/3}, \quad (73)$$

where D is a constant and scale invariant.

2.2 Properties of the figure-eight solution

The figure-eight solution is a solution of the equation of motion (5). The three bodies chase each other on the same single orbit that looks like “8” with equal time spacing. Namely, for period T , the solution $q_k(t)$ is described by a single function $q(t)$,

$$q_k(t) = q \left(t + \frac{kT}{3} \right), \text{ for } k = 0, 1, 2. \quad (74)$$

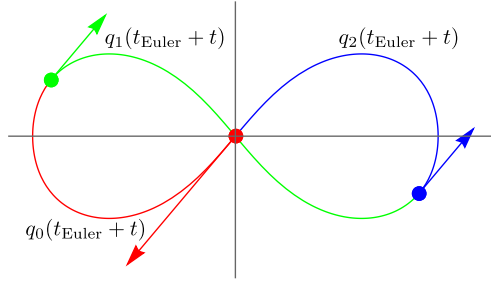


Figure 5: Euler configuration and orbits of the figure-eight solution. Red, green, blue points represent $q_k(t_{\text{Euler}})$, $k = 0, 1, 2$ respectively. Curves represent the orbit $q_k(t_{\text{Euler}} + t)$, for $t \in [0, T/3]$.

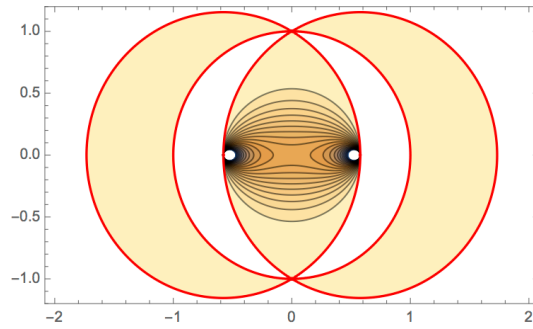


Figure 6: The potential function μ in $\alpha = 2$ for $\eta = x + iy$ on the path $z = t_{\text{Euler}} + i\tau$. The red circles represent the contours for $\mu = 0$ and the colored region represents $\mu > 0$.

The center of mass and the total momentum is set to zero,

$$\sum q_k = \sum p_k = 0 \text{ and similar equations for } \tilde{q}_k, \tilde{p}_i. \quad (75)$$

Since the left and right lobe of the orbit has the same area with opposite direction, the solution has vanishing angular momentum,

$$\sum \left(x_k \frac{dy_k}{dt} - y_k \frac{dx_k}{dt} \right) = 0. \quad (76)$$

The figure-eight solution takes Euler configurations and isosceles configurations alternately in the interval $T/12$. In the following sections, the behavior of the figure-eight solution around an Euler configuration and an isosceles configuration will be discussed.

2.2.1 Around an Euler configuration

The figure-eight solution has 6 Euler configurations when one body is at the origin and momenta of other two bodies are equal. Figure 5 represents one of the Euler configurations when $q_0 = 0$ and $dq_1/dt = dq_2/dt$. Let this moment be $t = t_{\text{Euler}}$.

Since at $t = t_{\text{Euler}}$, $q_0 = 0$, $q_1 = -q_2$ and $p_1 = p_2$, the time reversal and index change $0 \rightarrow 0$, $1 \leftrightarrow 2$ is equivalent to the rotation of 180 degree around the origin. Nemely,

$$\begin{aligned} q_0(t_{\text{Euler}} - t) &= -q_0(t_{\text{Euler}} + t), \\ q_1(t_{\text{Euler}} - t) &= -q_2(t_{\text{Euler}} + t), \text{ and } q_2(t_{\text{Euler}} - t) = -q_1(t_{\text{Euler}} + t). \end{aligned} \quad (77)$$

Analytic continuation keeps this relations

$$\begin{aligned} q_0(t_{\text{Euler}} - z) &= -q_0(t_{\text{Euler}} + z), \\ q_1(t_{\text{Euler}} - z) &= -q_2(t_{\text{Euler}} + z), \text{ and } q_2(t_{\text{Euler}} - z) = -q_1(t_{\text{Euler}} + z) \end{aligned} \quad (78)$$

for $z \in \mathbb{C}$ in some region including the real axis.

Let $t, \tau \in \mathbb{R}$. Since $\tilde{q}_k(z) = (q_k(z^*))^*$ in this region and by (78),

$$\tilde{q}_0(t_{\text{Euler}} - t + i\tau) = (q_0(t_{\text{Euler}} - t - i\tau))^* = -(q_0(t_{\text{Euler}} + t + i\tau))^*. \quad (79)$$

Similarly,

$$\tilde{q}_1(t_{\text{Euler}} - t + i\tau) = -(q_2(t_{\text{Euler}} + t + i\tau))^*, \quad \tilde{q}_2(t_{\text{Euler}} - t + i\tau) = -(q_1(t_{\text{Euler}} + t + i\tau))^*. \quad (80)$$

For the shape variable, it follows

$$\tilde{\eta}(t_{\text{Euler}} - t + i\tau) = -(\eta(t_{\text{Euler}} + t + i\tau))^*. \quad (81)$$

Finally, for the path $z = t_{\text{Euler}} + i\tau$,

$$\tilde{q}_0 = -(q_0)^*, \quad \tilde{q}_1 = -(q_2)^*, \quad \tilde{q}_2 = -(q_1)^*, \quad (82)$$

and

$$\tilde{\eta} = -(\eta)^*. \quad (83)$$

Let $\eta = x + iy$, $x, y \in \mathbb{R}$ on this path. Then $\tilde{\eta} = -(\eta)^* = -(x - iy)$. Then the kinetic energy is given by

$$K = (1 + \eta\tilde{\eta})^{-2} \frac{d\eta}{dz} \frac{d\tilde{\eta}}{dz} = (1 - x^2 - y^2)^{-2} \left(\left(\frac{dx}{d\tau} \right)^2 + \left(\frac{dy}{d\tau} \right)^2 \right). \quad (84)$$

The potential function for $\alpha = 2$ is

$$\mu = \frac{(1 - x^2 - y^2) ((x - 1/\sqrt{3})^2 + y^2 - 4/3) ((x + 1/\sqrt{3})^2 + y^2 - 4/3)}{((x - 1/\sqrt{3})^2 + y^2) ((x + 1/\sqrt{3})^2 + y^2)}. \quad (85)$$

Therefore, the sign of μ for $\alpha = 2$ will change on three circles $x^2 + y^2 = 1$ and $(x \pm 1/\sqrt{3})^2 + y^2 = 4/3$. Since, the kinetic energy $K \geq 0$ in the region $x^2 + y^2 < 1$ and $K = \mu$ for periodic solution in $\alpha = 2$, the potential function μ must be positive or zero. Therefore, the orbit of η and $\tilde{\eta}$ on this path must be confined in the first region that contains the origin. See figure 6.

2.2.2 Around an isosceles configuration

The figure-eight solution has 6 isosceles configurations when one body is on the x-axis and other two bodies are mutually opposite side of the x-axis. Figure 7 represents one of the isosceles configurations when q_0 is on the x-axis and $x_1 = x_2$, $y_1 = -y_2$. Let this moment be $t = t_{\text{iso}}$.

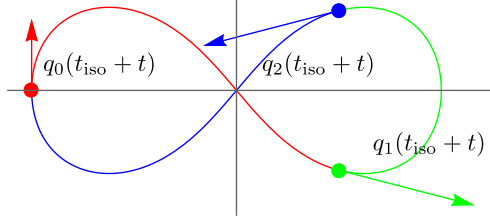


Figure 7: Isosceles configuration at $t = t_{\text{iso}}$ when the point q_0 is on the x-axis, and orbits of the figure-eight solution. Red, green, blue points represent $q_k(t_{\text{iso}})$, $k = 0, 1, 2$ respectively. Curves represent the orbit $q_k(t_{\text{iso}} + t)$ for $t \in [0, T/3]$.

Since time inversion at $t = t_{\text{iso}}$ and exchange of the index $1 \leftrightarrow 2$ is equivalent to the inversion with respect to the x-axis, namely,

$$\begin{aligned} x_0(t_{\text{iso}} - t) &= x_0(t_{\text{iso}} + t), \\ x_1(t_{\text{iso}} - t) &= x_2(t_{\text{iso}} + t), \text{ and } x_2(t_{\text{iso}} - t) = x_1(t_{\text{iso}} + t), \end{aligned} \quad (86)$$

and

$$\begin{aligned} y_0(t_{\text{iso}} - t) &= -y_0(t_{\text{iso}} + t), \\ y_1(t_{\text{iso}} - t) &= -y_2(t_{\text{iso}} + t), \text{ and } y_2(t_{\text{iso}} - t) = -y_1(t_{\text{iso}} + t). \end{aligned} \quad (87)$$

Since $x_0(t_{\text{iso}} + t)$ is an even function of t , $x_0(t_{\text{iso}} + i\tau)$ is real. Also, $y_0(t_{\text{iso}} + t)$ is an odd function of t , $y_0(t_{\text{iso}} + i\tau)$ is pure imaginary. For $z = t_{\text{iso}} + i\tau$, let $x_0 = x$ and $y_0 = iy$, $x(\tau), y(\tau) \in \mathbb{R}$. Then, for $z = t_{\text{iso}} + i\tau$

$$\begin{aligned} q_0(z) &= x_0(z) + iy_0(z) = x(z) - y(z) \in \mathbb{R}, \\ \tilde{q}_0(z) &= x_0(z) - iy_0(z) = x(z) + y(z) \in \mathbb{R}. \end{aligned} \quad (88)$$

On the other hand,

$$\begin{aligned} (x_1(t_{\text{iso}} + i\tau))^* &= (x_2(t_{\text{iso}} - i\tau))^* = x_2^\dagger(t_{\text{iso}} + i\tau) = x_2(t_{\text{iso}} + i\tau), \\ (y_1(t_{\text{iso}} + i\tau))^* &= -(y_2(t_{\text{iso}} - i\tau))^* = -y_2^\dagger(t_{\text{iso}} + i\tau) = -y_2(t_{\text{iso}} + i\tau) \end{aligned} \quad (89)$$

yields

$$(x_1(t_{\text{iso}} + i\tau))^* \mp i(y_1(t_{\text{iso}} + i\tau))^* = x_2(t_{\text{iso}} + i\tau) \pm iy_2(t_{\text{iso}} + i\tau). \quad (90)$$

Namely, for $z = t_{\text{isosceles}} + i\tau$

$$(q_1(z))^* = q_2(z) \text{ and } (\tilde{q}_1(z))^* = \tilde{q}_2(z). \quad (91)$$

Therefore, for some interval of τ , q_0 are on the real axis and q_1 and q_2 are mutually complex conjugate. So, the triangle $q_0q_1q_2$ remains to be an isosceles triangle.

Then, the shape variable η is pure imaginary,

$$\eta = \frac{\sqrt{3} q_0}{q_2 - q_1} = \frac{\sqrt{3} q_0}{(q_1)^* - q_1} \in i\mathbb{R}. \quad (92)$$

Therefore, it is natural to define

$$\eta(t_{\text{iso}} + i\tau) = i\zeta(\tau), \quad \zeta \in \mathbb{R}. \quad (93)$$

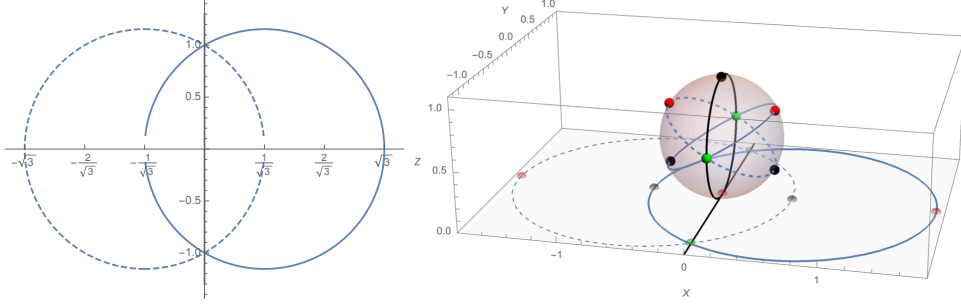


Figure 8: Three circles in the shape plane η (left) and shape sphere (right). The y-axis, the solid circle, the dashed circle on the shape plane represent $\eta = i\zeta$ ($\zeta \in \mathbb{R}$), $|\eta - 1/\sqrt{3}| = 2/\sqrt{3}$, and $|\eta + 1/\sqrt{3}| = 2/\sqrt{3}$ respectively. The points $\pm\infty$, $-1/\sqrt{3}$, and $+1/\sqrt{3}$ represent the collision of $q_1 - q_2 \rightarrow 0$, $q_0 - q_1 \rightarrow 0$, and $q_0 \rightarrow q_2$. The three circles on the shape plane correspond to the great circles of longitude 0 , $2\pi/3$, and $4\pi/3$ on the shape sphere. The points 0 and $\pm\sqrt{3}$ stands for Euler points, and the points ± 1 for Lagrange points.

For the other isosceles configuration at $t = t_{\text{iso}} + T/3 + t$, $q_k(t_{\text{iso}} + T/3 + t) = q_{k+1}(t_{\text{iso}} + t)$ make the cyclic permutation of indexes $0 \rightarrow 1 \rightarrow 2 \rightarrow 0$. Therefore, using (47),

$$\eta(t_{\text{iso}} + T/3 + i\tau) = \frac{\sqrt{3} + i\zeta(\tau)}{1 - i\sqrt{3}\zeta(\tau)} = \frac{1}{\sqrt{3}} + \frac{2}{\sqrt{3}} \left(\frac{1 + i\sqrt{3}\zeta(\tau)}{1 - i\sqrt{3}\zeta(\tau)} \right). \quad (94)$$

and using the same permutation again,

$$\eta(t_{\text{iso}} + 2T/3 + i\tau) = -\frac{\sqrt{3} - i\zeta(\tau)}{1 + i\sqrt{3}\zeta(\tau)} = -(\eta(t_{\text{iso}} + T/3 + i\tau))^*. \quad (95)$$

Namely, in the complex plane, $\eta(t_{\text{iso}} + i\tau)$ is on the y-axis and $\eta(t_{\text{iso}} + T/3 + i\tau)$ and $\eta(t_{\text{iso}} + 2T/3 + i\tau)$ are on each circle whose radius is $2/\sqrt{3}$ and whose center is $1/\sqrt{3}$ and $-1/\sqrt{3}$ respectively. Similarly, $\tilde{\eta}(t_{\text{iso}} + i\tau)$ is also pure imaginary. There is no obvious relation between $\eta(t_{\text{iso}} + i\tau)$ and $\tilde{\eta}(t_{\text{iso}} + i\tau)$. They are two independent variables.

More about q_k : Let $q_0 = -2a$, $q_1 = a - ib$, $q_2 = a + ib$ and $\tilde{q}_0 = -2\alpha$, $\tilde{q}_1 = \alpha + i\beta$, $q_2 = \alpha - i\beta$. Then, the moment of inertia is

$$r^2 = q_0\tilde{q}_0 + q_1\tilde{q}_1 + q_2\tilde{q}_2 = 6a\alpha + 2b\beta = \text{constant}. \quad (96)$$

The equation for vanishing angular momentum yield

$$\sum q_k \frac{d\tilde{q}_k}{dz} - \tilde{q}_k \frac{dq_k}{dz} = 6 \left(a \frac{d\alpha}{dz} - \alpha \frac{da}{dz} \right) + \left(b \frac{d\beta}{dz} - \beta \frac{db}{dz} \right) = 0. \quad (97)$$

So, we still have two independent variables.

In this parametrization, the shape variables $\bar{\eta} = i\sqrt{3}a/b$ and $\tilde{\eta} = -i\sqrt{3}\alpha/\beta$. Then,

$$\eta\tilde{\eta} = \frac{3a\alpha}{b\beta} = \frac{r^2 - 2b\beta}{2b\beta}. \quad (98)$$

Therefore, $\eta\tilde{\eta} \rightarrow -1$ if $b\beta \rightarrow \infty$.

3 Numerical integrations by Mathematica

3.1 Integrations for complex variables on complex path

Mathematica can treat differential equations $df_n(t)/dt = g_n(t)$ for complex variables f_n and g_n . However, the independent variable t must be real.

So, to integrate the equations of motion for $z = z_i$ to z_f , we take a complex number e that is proportional to $z_f - z_i$. Then, using $dz = ed\sigma$, $\sigma \in \mathbb{R}$, we rewrite the equations of motion in the following,

$$\begin{aligned} \frac{dq_k}{d\sigma} &= e \frac{\partial \mathcal{H}}{\partial p_k}, & \frac{d\tilde{p}_i}{d\sigma} &= -e \frac{\partial \mathcal{H}}{\partial \tilde{q}_k}, \\ \frac{d\tilde{q}_k}{d\sigma} &= e \frac{\partial \mathcal{H}}{\partial \tilde{p}_i}, & \frac{dp_k}{d\sigma} &= -e \frac{\partial \mathcal{H}}{\partial q_k}. \end{aligned} \quad (99)$$

There are two choices for e and σ , 1) $e = (z_f - z_i)/|z_f - z_i|$ and $\sigma \in [0, |z_f - z_i|]$, 2) $e = z_f - z_i$ and $\sigma \in [0, 1]$. I'm using both.

3.2 Method to take a proper branch in the equation of motion

For any multivalued function, Mathematica returns a principal value that is defined by the Wolfram language. This can make artificial discontinuity when the denominator in the equation of motion $((q_j - q_k)(\tilde{q}_j - \tilde{q}_k))^{\alpha/2+1}$ passes through the branch cut.

There is no problem for $\alpha = 2$ and 0 . The terms are $((q_j - q_k)(\tilde{q}_j - \tilde{q}_k))^2$ and $(q_j - q_k)(\tilde{q}_j - \tilde{q}_k)$.

For $\alpha = 1$, Newton potential, the denominator in the equation of motion is $((q_j - q_k)(\tilde{q}_j - \tilde{q}_k))^{3/2}$. In this case, we can introduce three auxiliary variables $r_{ij}(z)$ that stand for $((q_j - q_k)(\tilde{q}_j - \tilde{q}_k))^{1/2}$ and make the equations of motion

$$\begin{aligned} \frac{dq_k}{d\sigma} &= e \tilde{p}_i, & \frac{d\tilde{p}_i}{d\sigma} &= e \sum_j \frac{q_j - q_k}{r_{jk}^3}, \\ \frac{d\tilde{q}_k}{d\sigma} &= e p_k, & \frac{dp_k}{d\sigma} &= e \sum_j \frac{\tilde{q}_j - \tilde{q}_k}{r_{jk}^3}, \\ \frac{dr_{ij}}{d\sigma} &= \frac{1}{2r_{ij}} \left(\left(\frac{dq_i}{d\sigma} - \frac{dq_j}{d\sigma} \right) (\tilde{q}_i - \tilde{q}_j) + (q_i - q_j) \left(\frac{d\tilde{q}_i}{d\sigma} - \frac{d\tilde{q}_j}{d\sigma} \right) \right). \end{aligned} \quad (100)$$

In the last equation, there is no e in the both side. I didn't do this calculation.

For general α , for example $\alpha = \sqrt{2}$, we can introduce additional three more auxiliary variables R_{ij} that stand for r_{ij}^α . Then we add the equations for R_{ij} ,

$$\frac{dR_{ij}}{d\sigma} = \frac{\alpha R_{ij}}{r_{ij}} \frac{dr_{ij}}{d\sigma}. \quad (101)$$

I didn't do this calculation.

3.3 Ask ‘‘NDSolve’’ to warm ‘‘an egg’’ with ‘‘other eggs’’

In this section, a tip to integrate a function of orbit $q(t)$ and $p(t)$ that are a solution of an equation of motion is described. For example, how to calculate the action variable J with very high accuracy,

$$J = \int_0^T \sum p_k(t) \tilde{p}_i(t) dt. \quad (102)$$

Here is my method. *I'm not sure this is the best or not.* Just give the differential equation for J (“an egg”) to “NDSolve” as well as the equations of motion (“other eggs”),

$$\frac{dq}{dt} = \frac{\partial H}{\partial p}, \frac{dp}{dt} = -\frac{\partial H}{\partial q}, \text{ and } \frac{dJ}{dt} = \sum p_k(t)\tilde{p}_i(t) \quad (103)$$

with initial condition $J(0) = 0$. Then, “NDSolve” will integrate this equations and gives us $J = J(T)$ with accuracy we want.

Professor Andrzej J. Maciejewski told me another method at the seminar. Add an option “InterpolationOrder -> All” to “NDSolve”. This works fine. Thanks.

Background: “NDSolve” of Mathematica gives an interpolating function $q(t)$ and $p(t)$. In my experiences, we can control the accuracy of the end point, $q(t_f)$ and $p(t_f)$ choosing the option parameters “WorkingPrecision”, “AccuracyGoal” and “PrecisionGoal”. So, we can get $q(t_f)$ and $p(t_f)$ with very high accuracy. However, the accuracy at intermediate time, $0 < t < t_f$ are poor. In my experiences, it is order 10^{-8} or something. So, even if we calculate $q(t)$ and $p(t)$ very accurately by NDSolve, the integration using “NIntegrate” gives the value with accuracy of order 10^{-8} or something. The two method shown above resolve this issue.

4 Numerical calculations for $\alpha = 2$, a strong force potential

4.1 The initial conditions and the accuracy

We fixed the period $T = 1$. The initial condition for the isosceles configuration with 40 digits is

$$q_0 = 0.19743123404582463292775384213515165845219778006226 \\ + 0.15377830312582075297746703903968385700658995175922i \quad (104)$$

It takes 0.83 sec to calculate $t \in [0, T/12]$. The values at $t = T/12$ that must be 0 represent an order of accuracy.

$$q_0(T/12) = 2.9 \times 10^{-25} + 2.7 \times 10^{-26}i, \\ p_1[T/12] - p_2[T/12] = -6.6 \times 10^{-24} - 5.0 \times 10^{-24}i. \quad (105)$$

Using the same initial conditions, the calculation for $t \in [0, T]$ takes 9.28 sec. The periodicity that should be 0 also represent an order of accuracy squared.

$$\sum (q_k(T) - q_k(0))(\tilde{q}_k(T) - \tilde{q}_k(0)) = 5.2 \times 10^{-40}, \\ \sum (p_k(T) - p_k(0))(\tilde{p}_i(T) - \tilde{p}_i(0)) = 1.4 \times 10^{-37}. \quad (106)$$

So, we can trust this numerical calculation with accuracy of order 10^{-18} .

4.2 Overview of the singularities

Using the initial condition, we calculated the function $q(z) = q_0(z)$ in the complex plane. The integration path to $z = t + i\tau$ was taken $z = 0 \rightarrow t \rightarrow t + i\tau$.

We can see singularities at $\Re(z) = 1/12 + k/6$, $k = 1, 2, 3, \dots, 6$, $\Im(z) \sim \pm 0.1$, see figure 9.

In the region that contains the real axis and not contains any singularities, the function $q_k(z), \tilde{q}_k(z), p_k(z), \tilde{p}_i(z)$ are analytic. Therefore the periodicity $q_k(z) = q_k(z + T)$ keeps. Then, for a small fixed τ , curve $q_k(t + i\tau)$, $t \in [0, T]$ in the complex plane make an closed loop. For

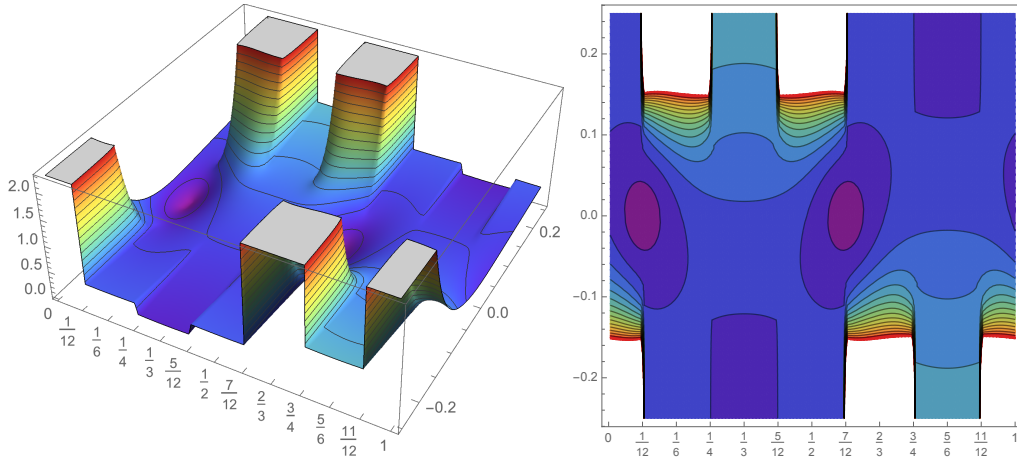


Figure 9: The absolute value of $q(z)$ for the figure-eight solution for $\alpha = 2$. The left is a 3D plot. The x and y direction is t and τ for $z = t + i\tau$ and the vertical direction is $|q(z)|$. Values $|q(z)| > 2$ are cut off. The right is a contour plot for the same values. We can see singularities at $z = 1/12 + k/6 \pm i\tau_0$, $k = 1, 2, 3, 4, 5, 6$ and $\tau_0 \sim 0.09$.

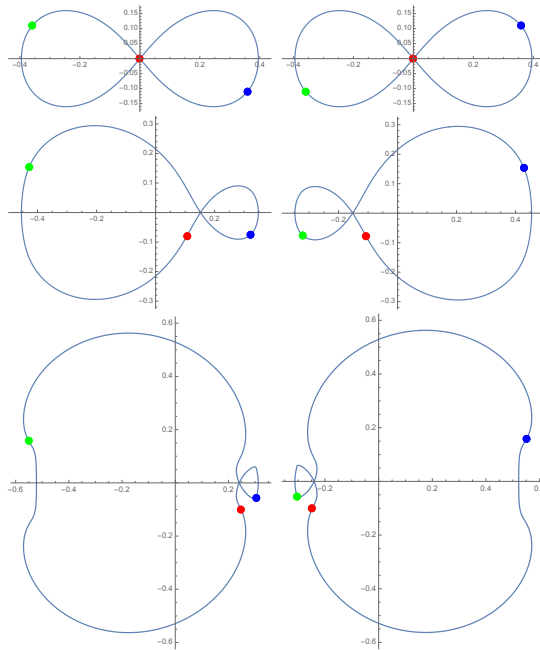


Figure 10: Deformations by τ of the figure-eight solution for $\alpha = 2$. The left column: $q(t + i\tau)$ for $t \in [0, T]$. Top to down, $\tau = 0, 0.05, 0.09$. The right column: Same for $\tilde{q}(t + i\tau)$. Red, green, blue points represent the body 0, 1, 2 respectively.

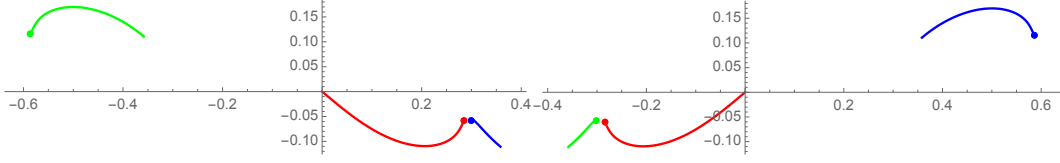


Figure 11: Figure-eight solution for $\alpha = 2$: $q(1/12 + i\tau)$ (left) and $\tilde{q}(1/12 + i\tau)$ (right) for $\tau \in [0, 0.09]$. Red, green, blue points represent the body 0, 1, 2 respectively. Edges without point represent $\tau = 0$, while with point represent $\tau = 0.09$.

$\tau = 0$, this loop is the figure-eight. Making the value of τ slightly large, the curve $q_k(t+i\tau)$ is also a closed curve, namely, a slightly deformed figure-eight. Larger value of τ makes a deformation large. Then, near $\tau \sim 0.1$, something singular will happen. See figure 10.

To see what is happened near a singularity, we trace the behavior of $q(z)$ for $z = 1/12 \rightarrow 1/12 + 0.09i$. See figure 11. What we can see from the figure 11 is $z = 1/12 + i\tau$, $\tau \in \mathbb{R}$,

$$\tilde{q}_0(z) = -(q_0(z))^*, \quad \tilde{q}_1(z) = -(q_2(z))^*, \quad \tilde{q}_2(z) = -(q_1(z))^*, \quad (107)$$

that is shown in (82).

4.3 A “half collision”

The other thing we can see from the figure 11 is, for $z \rightarrow z_0$: singularity, **the functions looks to behave**.

$$\begin{aligned} q_0(z), q_2(z) &\rightarrow Q \quad \therefore q_1(z) \rightarrow -2Q, \\ \tilde{q}_0(z), \tilde{q}_1(z) &\rightarrow -Q^* \quad \therefore \tilde{q}_2(z) = 2Q^*. \end{aligned} \quad (108)$$

This is a simultaneous “half collision”.

If the simultaneous “half collision” (108) really takes place, the moment of inertia I is $I = \sum_k q_k \tilde{q}_k \rightarrow 3QQ^*$. Therefore,

$$QQ^* \rightarrow \frac{I}{3}. \quad (109)$$

And the shape variables behave

$$\begin{aligned} \eta &= \frac{\sqrt{3}q_0}{q_2 - q_1} \rightarrow \frac{\sqrt{3}Q}{Q + 2Q} = \frac{1}{\sqrt{3}}, \\ \tilde{\eta} &= \frac{\sqrt{3}\tilde{q}_0}{\tilde{q}_2 - \tilde{q}_1} \rightarrow \frac{-\sqrt{3}Q^*}{2Q^* + Q^*} = -\frac{1}{\sqrt{3}}. \end{aligned} \quad (110)$$

This limit value $\pm 1/\sqrt{3}$ gives the singular points of the shape potential $\mu(\eta, \tilde{\eta})$,

$$\mu(\eta, \tilde{\eta}) = \left(\frac{1 + \eta\tilde{\eta}}{2} \right) \left(1 + \frac{4}{(1 - \sqrt{3}\eta)(1 - \sqrt{3}\tilde{\eta})} + \frac{4}{(1 + \sqrt{3}\eta)(1 + \sqrt{3}\tilde{\eta})} \right). \quad (111)$$

endif.

4.4 Behavior of the shape variables

Then, let us investigate the behavior of $\eta(z)$, $\tilde{\eta}(z)$ more precisely.

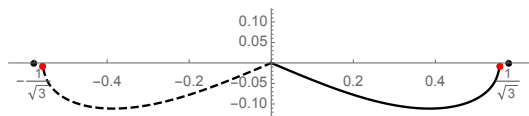


Figure 12: Figure-eight solution for $\alpha = 2$: Behavior of the shape variables $\eta(1/12 + i\tau)$ and $\tilde{\eta}(1/12 + i\tau)$. The solid curve represents η , the dashed $\tilde{\eta}$. The red points represents the values at $\tau = 0.09$. The black points stands for $\pm 1/\sqrt{3}$. The red and black points are definitely separated.

4.4.1 For the path $z = 0 \rightarrow 1/12$ (Euler config.) $\rightarrow 1/12 + i\tau$

On this path, *the speculation (110) is doubtful*. It may be wrong. Figure 12 shows the behavior of $\eta(z)$ and $\tilde{\eta}(z)$ integrated on the path $z = 0 \rightarrow 1/12 \rightarrow 1/12 + 0.09i$ and shown for the interval $z = 1/12 \rightarrow 1/12 + 0.09i$. Although the point $z = 1/12 + 0.09i$ is considerably close the singular point, figure 12 shows that the variables η and $\tilde{\eta}$ are definitely separated from the singular points $\eta = 1/\sqrt{3}$, $\tilde{\eta} = -1/\sqrt{3}$ and not look like to come to the singular point. The right red point is $0.5577\dots - 0.00696\dots i$, while the black point, the singular point of the potential is $1/\sqrt{3} = 0.577\dots$. The separation is 0.02. This is clearly not zero in this precision.

On the other hand, the relations (107) is correct on this path. Therefore, the relation for η and $\tilde{\eta}$ is

$$\tilde{\eta} = \frac{\sqrt{3} \tilde{q}_0}{\tilde{q}_2 - \tilde{q}_1} = \frac{\sqrt{3} (-q_0^*)}{-q_1^* + q_2^*} = -(\eta)^*. \quad (112)$$

This is the equation (83) which can be validated by figure 12.

4.4.2 For the path $z = 0 \rightarrow 1/12 \pm \epsilon \rightarrow 1/12 \pm \epsilon + i/10$

Then, we calculate η and $\tilde{\eta}$ for the path $z \rightarrow 1/12 \pm \epsilon \rightarrow 1/12 \pm \epsilon + i/10$. The results are shown in the figure 13.

(WorkingPrecision=90, AccuracyGoal=PrecisionGoal=70)

Figure 13 clearly show that $\eta(1/12 + \epsilon + i\tau)$ passes through the singular point $1/\sqrt{3}$ for some value of $\epsilon \in [0, 1/1000]$. However, for the same value of ϵ , $\tilde{\eta}$ doesn't pass the singular point $-1/\sqrt{3}$.

Namely, *figure-eight solution with $\alpha = 2$ doesn't have simultaneous "half collision"*. A "half collision" $\eta(z) \rightarrow 1/\sqrt{3}$ takes place on the line slightly right of $\Re(z) = 1/12$, while a "half collision" $\tilde{\eta}(z) \rightarrow -1/\sqrt{3}$, takes place slightly left of $\Re(z) = 1/12$.

The orbit of η and $\tilde{\eta}$ for the line $\Re(z) = 1/12$ in the figure 13 have bounce near $(\pm 1/\sqrt{3}, 0)$. These bounces are due to the potential barrier. See figure 6. The orbits are confined in the first region that contains the origin in the figure 6.

4.4.3 For the path $z = 0 \rightarrow k/6$ (isosceles) $\rightarrow k/6 + i\tau$

The points $z = k/6$, $k = 0, 1, 2$ are isosceles configurations.

See figure 14. For the path $z = k/6$ (isosceles) $\rightarrow k/6 + i\tau$ for $k = 0, 1, 2, \dots$, $\tau \in \mathbb{R}$, the triangle $q_0 q_1 q_2$ keeps isosceles triangle. 1) For the path $k = 0$, it looks like $q_0 - q_2 \rightarrow 0$ and $\tilde{q}_0 - q_2 \rightarrow \infty$ for $\tau \rightarrow \infty$. So, $\eta \rightarrow 1/\sqrt{3}$ and $\tilde{\eta} \rightarrow -1/\sqrt{3}$. 2) For the path $k = 2$, $q_1 - q_2 \rightarrow 0$ and it looks like $\tilde{q}_1 - \tilde{q}_2 \rightarrow \infty$. It looks like $\eta \rightarrow$ a large finite and $\tilde{\eta} \rightarrow$ a small finite.

The two observation 1) and 2) for $\eta, \tilde{\eta}$ are inconsistent. If $\eta \rightarrow \pm 1/\sqrt{3}$ for some k , the η must be one of $\pm 1/\sqrt{3}$ or ∞ for any k . And, if $\eta \rightarrow \infty$ in some k , the η must be one of $\pm 1/\sqrt{3}$ or ∞ for any k .

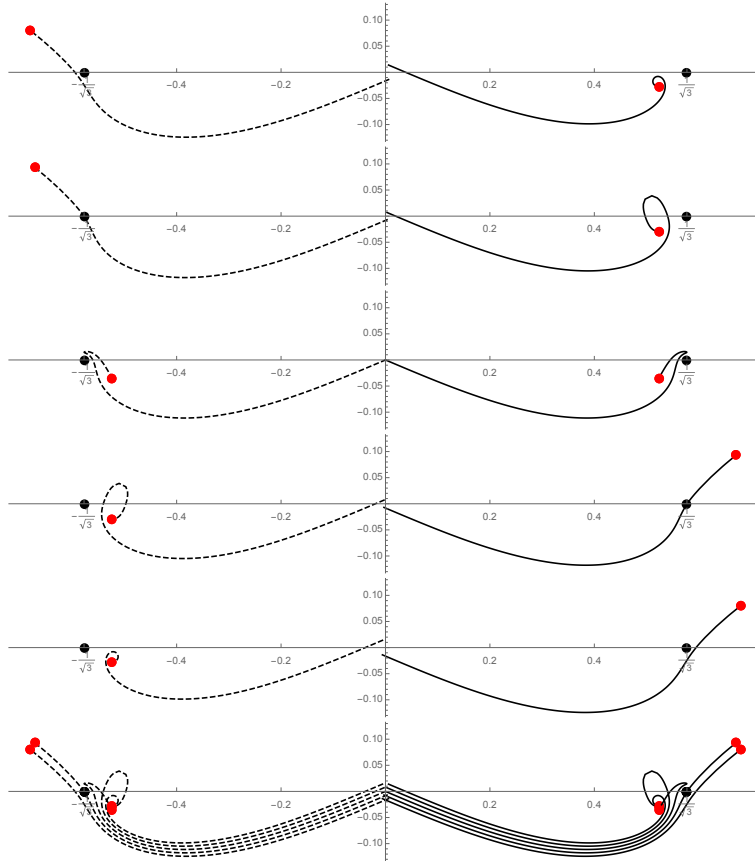


Figure 13: Figure-eight solution for $\alpha = 2$: The behavior of η and $\tilde{\eta}$ on the path $z \rightarrow 1/12 + \epsilon \rightarrow 1/12 + \epsilon + i/10$. From the top to bottom $\epsilon = -2/1000, -1/1000, 0, 1/1000, 2/1000$, and the collection of them. Although the curve with $\epsilon = 0$ has sharp kink, neither η nor $\tilde{\eta}$ pass over the singular point $\pm 1/\sqrt{3}$. The curve for η on $\epsilon = 1/1000$, the 4th row, looks like pass over $1/\sqrt{3}$, however, it passes through the right side of the point by 0.00045. For $\tilde{\eta}$ on $\epsilon = -1/1000$, the second row, is the same. The curves are symmetric for the sign of ϵ by (81).

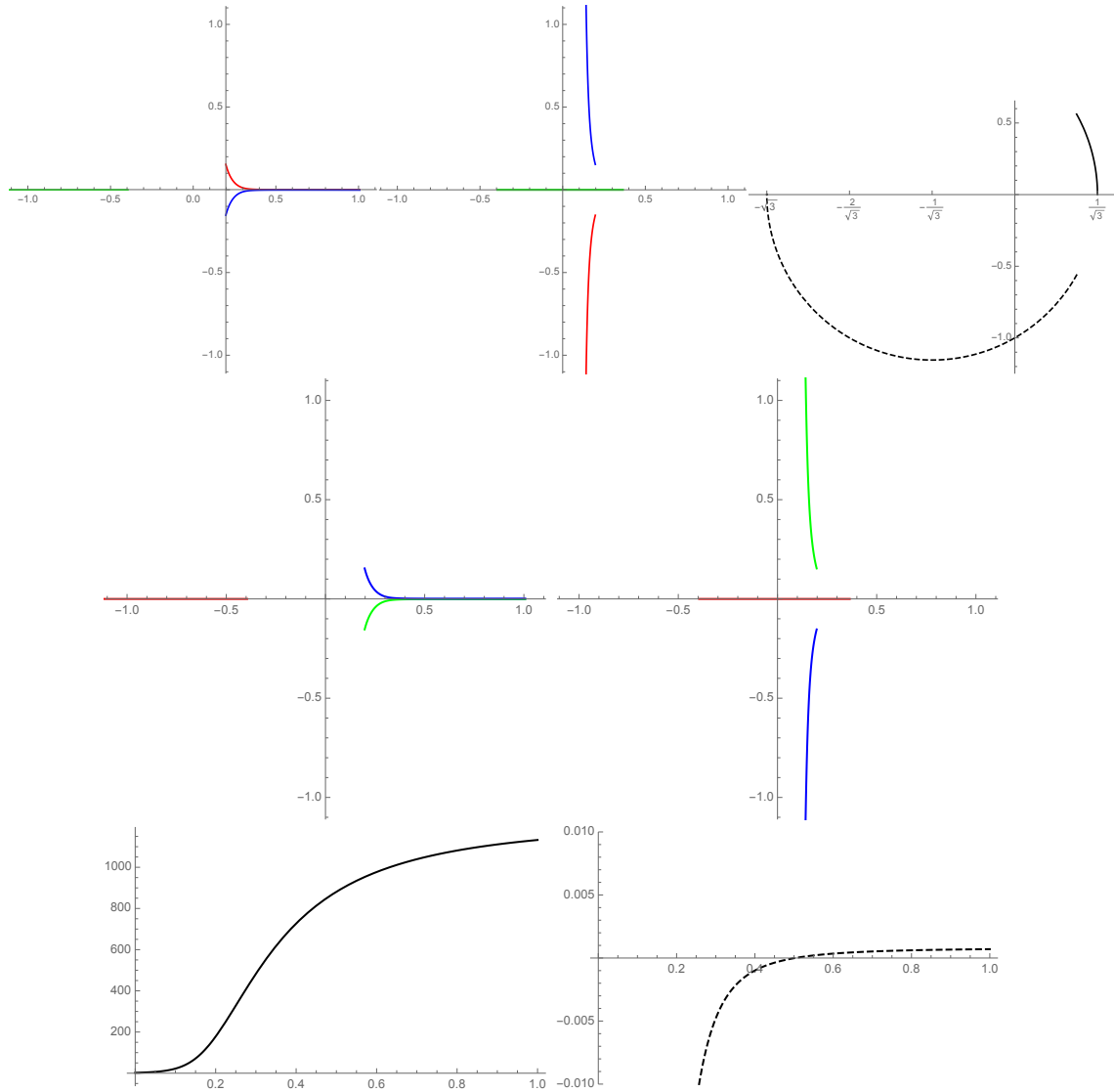


Figure 14: Figure-eight solution for $\alpha = 2$: Variables for the path $z = 0 \rightarrow k/6$ (isosceles) $\rightarrow k/6 + i$. Top row from left to right: $q_i(z)$, $\tilde{q}_i(z)$ and $\eta(z)$ (solid curve), $\tilde{\eta}(z)$ (dashed curve) for $k = 0$. Middle row from left to right: $q_i(z)$, $\tilde{q}_i(z)$ for $k = 2$. The bottom from left to right: $\Re(\eta(z))$ and $\Re(\tilde{\eta}(z))$ for $k = 2$.

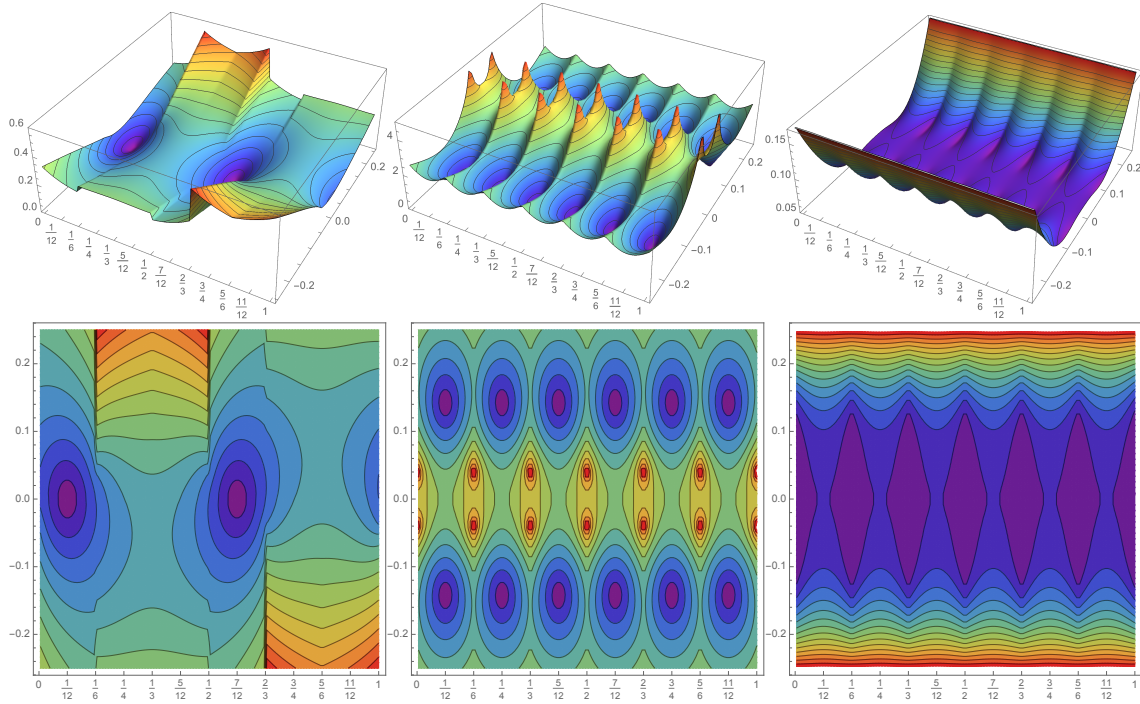


Figure 16: Figure-eight solution for $\alpha = 0$: The left column represents $|q(z)|$, the middle $|K(z)|$, and the right $|I(z)|$. The upper row is a 3D view, and the lower is a contour map.

5.2 Overview of the singularities

(The working precision is 50 digits, accuracy goal is 30 digits.) The singularities take place around $z = k/6 + i\tau$, $k = 1, 2, 3, \dots, 6$, $\tau \sim \pm 0.037$. At the time $t = k/6$, the configuration is isosceles.

Then, we investigate the behavior of q and \tilde{q} on the passes $0 \rightarrow 0.037i$ and $0 \rightarrow 1/6 \rightarrow 1/6 + 0.037i$. See figure 17 and 18.

For this logarithmic potential, q_0, q_2 look to behave $q_0, q_2 \rightarrow Q \in \mathbb{R}$ for $z = 0 \rightarrow 0.037i$. On this path, the relations $q_1(z), \tilde{q}_1(z) \in \mathbb{R}$, $(q_0)^* = q_2(z)$, $(\tilde{q}_0)^* = q_2(z)$ are satisfied. The behavior is completely different from that of $\alpha = 2$.

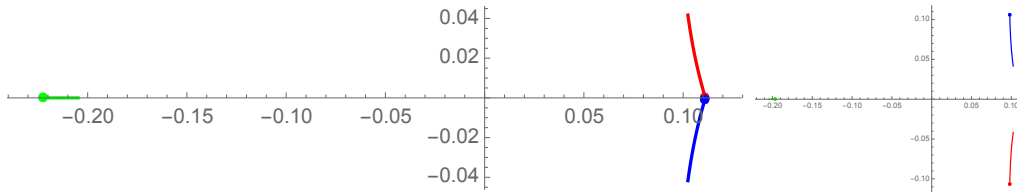


Figure 17: Figure-eight solution for $\alpha = 0$: $q_k(z)$ and $\tilde{q}_k(z)$ on the path $z = 0 \rightarrow 0.037i$. The edge with a point is $z = 0.037i$. Red, green, blue stand for 0, 1, 2 respectively. It looks like $q_0, q_3 \rightarrow Q \in \mathbb{R}$. $z = 0$ represents an isosceles configuration.

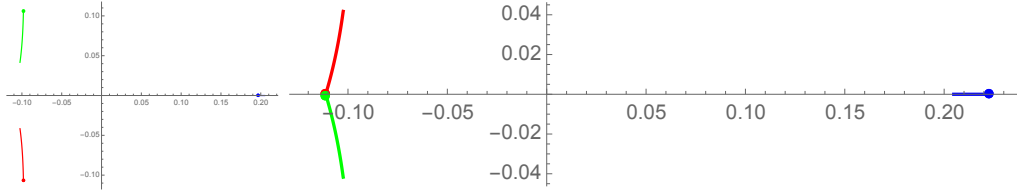


Figure 18: Figure-eight solution for $\alpha = 0$: $q_k(z)$ and $\tilde{q}_k(z)$ on the path $z = 0 \rightarrow 1/6 \rightarrow 1/6 + 0.037i$. The part of $z = 1/6 \rightarrow 1/6 + 0.037i$ is shown. The edge with a point is $z = 1/6 + 0.037i$. Red, green, blue stand for $k = 0, 1, 2$ respectively. On this path, it looks like $\tilde{q}_0, \tilde{q}_1 \rightarrow -Q$. $z = 1/6$ represents an isosceles configuration.

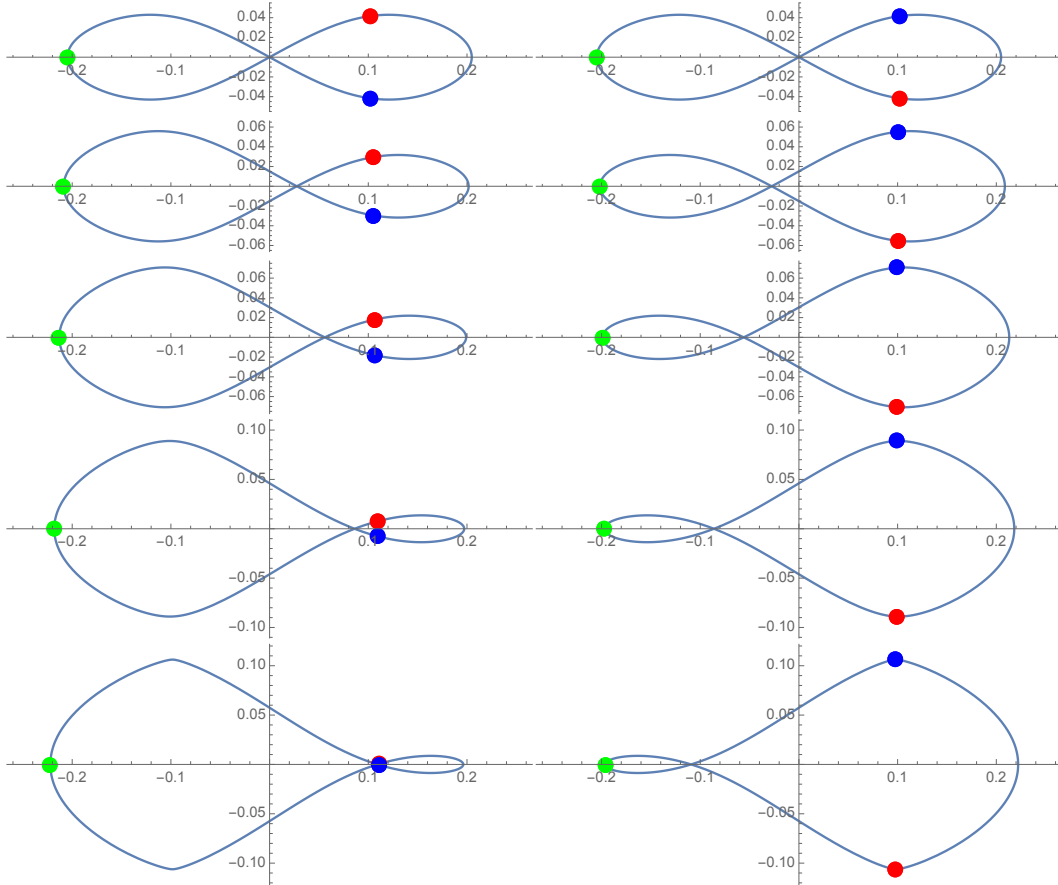


Figure 19: Figure-eight solution for $\alpha = 0$: Left and right column represent $q(t+i\tau)$ and $\tilde{q}(t+i\tau)$ respectively, for $t \in [0, T]$ with fixed τ . Top to down row represent $\tau = 0, 0.01, 0.02, 0.03$ and 0.037 . Red, green, blue points stand for $t = 0, T/3, 2T/3$.

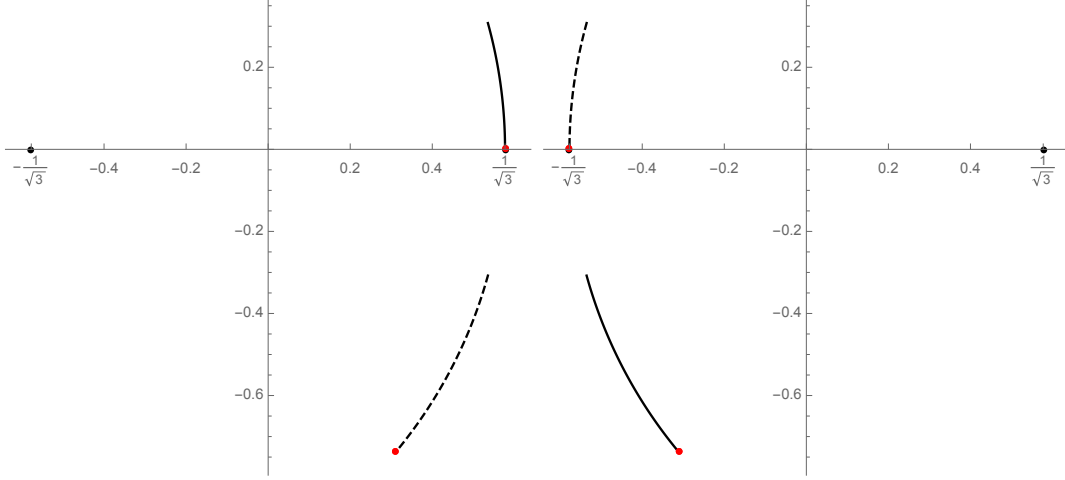


Figure 20: Figure-eight solution for $\alpha = 0$: $\eta(k/6 + i\tau)$ (solid curve) and $\tilde{\eta}(k/6 + i\tau)$ (dashed curve), $\tau \in [0, 0.037]$ for the figure-eight in logarithmic potential. The left stands for $k = 0$ and the right for $k = 1$. η goes to $1/\sqrt{3}$ in the left ($k = 0$), and $\tilde{\eta}$ goes to $-1/\sqrt{3}$ for the right ($k = 1$). The end point with red point stands for $\tau = 0.037$. For $k = 2$, η and $\tilde{\eta}$ are pure real, that is shown in figure 21. Configurations at $z = k/6$ for $k = 0, 1, 2, \dots$ represent isosceles configurations.

5.3 Behavior of the variables

5.3.1 For the path $z = 0 \rightarrow k/6$ (isosceles config.) $\rightarrow k/6 + i\tau$

We investigate η and $\tilde{\eta}$ on the path $z = 0 \rightarrow k/6 \rightarrow k/6 + 37i/1000$. The configurations at $z = k/6$, $k = 0, 1, 2, \dots$ are isosceles configurations. See figure 20. For $k = 0$, η goes to $1/\sqrt{3}$, while for $k = 1$, $\tilde{\eta}$ goes to $-1/\sqrt{3}$. The difference between η and the singular point at $\tau = 37/1000$ is $\eta(37i/1000) - 1/\sqrt{3} = -6.13 \times 10^{-6} + 0.00376i$. Thus, $\eta(z)$ goes to the singular point a little bit above $z = 37i/1000$.

As shown before, for $k = 2$, namely on the path $z = 1/3 \rightarrow 1/3 + i\tau$, η and $\tilde{\eta}$ are pure imaginary. The values are

$$\begin{aligned} \eta(1/3) &= -2.697 \times 10^{-50} + 4.2541239769777412027037212009155794354168623946363i, \\ \tilde{\eta}(1/3) &= -2.697 \times 10^{-50} - 4.2541239769777412027037212009155794354168623946363i, \end{aligned} \quad (117)$$

This must satisfy $\eta(1/3) + \tilde{\eta}(1/3) = 0$. And

$$\begin{aligned} \eta(1/3 + 0.00376i) &= 5 \times 10^{-47} + 354.39756079277408947472999964069417467817273118485i, \\ \tilde{\eta}(1/3 + 0.00376i) &= 0 \times 10^{-50} - 1.6001247850505522871270219532920776564783048707308i. \end{aligned} \quad (118)$$

See figure 21.

The orbits of $\eta(z)$, $\tilde{\eta}(z)$ for $z = \epsilon \rightarrow \epsilon + i\tau$, $\tau \in [0, 0.06]$ with $\epsilon = k/1000$, $k = -2, -1, 1, 2$, without $k = 0$ are shown in figure 22.

5.3.2 For the path $z = 0 \rightarrow 1/12$ (Euler config.) $\rightarrow 1/12 + 3i$

The configuration at $z = 1/12$ is an Euler configuration. The integration path is $z = 0 \rightarrow 1/12 \rightarrow 1/12 + 3i$. The figure 23 shows the behavior of q, \tilde{q}, η and $\tilde{\eta}$ for $z = 1/12 \rightarrow 1/12 + 3i$.

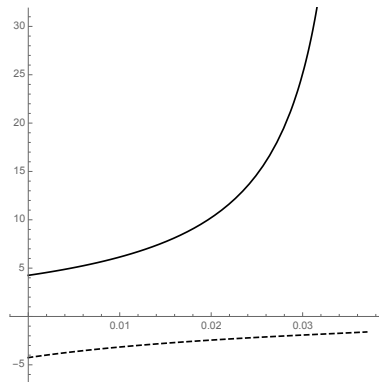


Figure 21: Figure-eight solution for $\alpha = 0$: The shape variables η and $\tilde{\eta}$ for $z = 1/3 \rightarrow 1/3 + 0.037i$. On this path, the variables are pure imaginary. Solid line represents $\Im(\eta)$ and dashed line $\Im(\tilde{\eta})$. At $z = 1/3$, $\eta + \tilde{\eta} = 0$. $\eta \rightarrow \infty$ for $z \rightarrow 1/3 + (0.037 + \dots)i$. Configuration at $z = 1/3$ is an isosceles configuration.

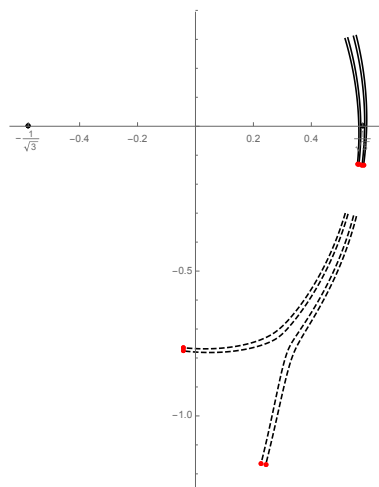


Figure 22: Figure-eight solution for $\alpha = 0$: The orbits of shape variables $\eta(z)$ (solid curve) and $\tilde{\eta}(z)$ (dashed curve) for the paths $z = \epsilon \rightarrow \epsilon + 0.6i$ with $\epsilon = k/1000$, $k = -2, -1, 1, 2$ without $k = 0$ are shown. The curves for right to left stand for $k = -2, -1, 1, 2$. Configuration at $z = 0$ is an isosceles configuration.

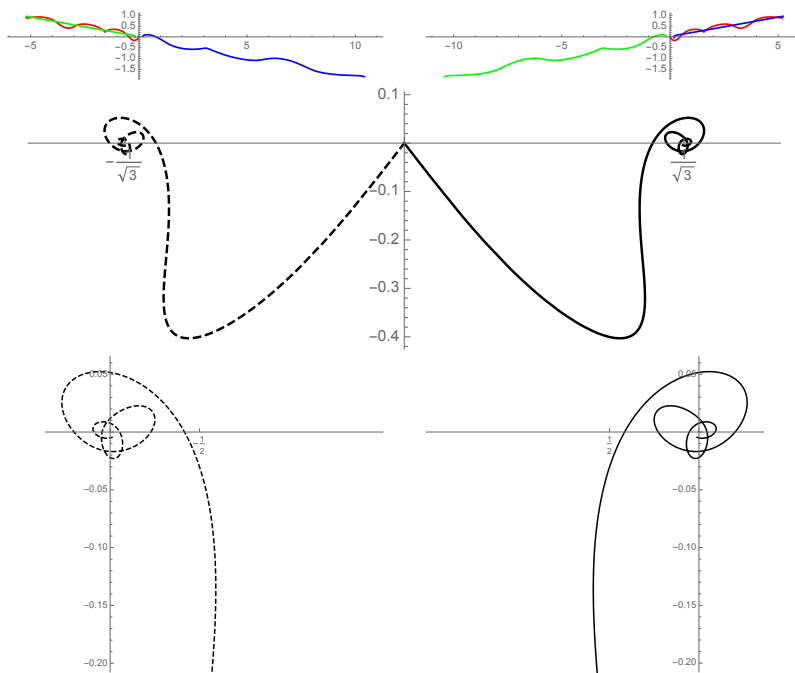


Figure 23: For the path $z = 1/12 \rightarrow 1/12 + i\tau$. The top row represents $\tilde{q}(z)$ (left) and $q(z)$ (right). The middle figure represents $\tilde{\eta}(z)$ (dashed curve) and $\eta(z)$ (solid). The bottom row shows closeup view of $\tilde{\eta}(z)$ (left) and $\eta(z)$ (right). In the lowest figures, the origin is $\pm 1/\sqrt{3}$.

On this path, q_0 and q_2 or \tilde{q}_0 and \tilde{q}_1 take “binary rotation”. For $\tau \rightarrow \infty$, it looks like $\eta \rightarrow 1/\sqrt{3}$ and $\tilde{\eta} \rightarrow -1/\sqrt{3}$ where “half collisions” take place.

6 Series expansion around a “collision” point

6.1 A “full collision”, “half collision”, and simultaneous “half collision”

In the real space-time, $t, x_k(t), y_k(t) \in \mathbb{R}$, a two-body collision take places when $x_i - x_j \rightarrow 0$ and $y_i - y_j \rightarrow 0$, equivalently $q_i - q_j \rightarrow 0$ and $\tilde{q}_i - \tilde{q}_j \rightarrow 0$ for $t \rightarrow t_0$. In this case, *both* $\eta, \tilde{\eta}$ tend to the *same* singular point $\pm 1/\sqrt{3}$ or ∞ . For example, *both* η and $\tilde{\eta}$ goes to $1/\sqrt{3}$. We would like call this case a “full collision” or “real collision”.

In the complex time z , however, it is possible to behave one of η or $\tilde{\eta}$ goes to a singular point while the other goes to normal point. For example, $\eta \rightarrow 1/\sqrt{3}$ and $\tilde{\eta} \rightarrow a \notin \{\pm 1/\sqrt{3}, \infty\}$. We will call this a “half collision”.

If two half collision take place for the same $z \rightarrow z_0$, we will call this a simultaneous “half collision”. For example, $\eta \rightarrow 1/\sqrt{3}$ and $\tilde{\eta} \rightarrow -1/\sqrt{3}$ for $z \rightarrow z_0$.

6.2 A series expansion around a possible simultaneous “half collision” for $\alpha = 2$

In this section, we will show that a possible simultaneous “half collision” on the path $z = t_{\text{Euler}} + i\tau$ does not behaves like the observation. In other words, the observed “half collision” are not simultaneous nor take place on the path $z = t_{\text{Euler}} + i\tau$. The half collisions take place at slightly different places, $z = t_{\text{Euler}} \pm \epsilon + i\tau_0$, $\epsilon \neq 0$, that is suggested by the numerical calculations.

Actually, we will show that possible simultaneous “half collision” on the path $z = t_{\text{Euler}} + i\tau$ for figure-eight solution in $\alpha = 2$ behaves

$$\eta = \frac{1}{\sqrt{3}}(1 - 2^{2/3}(\tau_0 - \tau)^{2/3} + \dots), \quad \tilde{\eta} = \frac{-1}{\sqrt{3}}(1 - 2^{2/3}(\tau_0 - \tau)^{2/3} + \dots) \quad (119)$$

for $\tau \rightarrow \tau_0 - 0$. So, the solution approaches the singular point from exactly left for η and from exactly right for $\tilde{\eta}$. This behavior is clearly different from the observed behavior. See figures 12 and 13.

The moment of inertia r^2 is constant for periodic solution in $\alpha = 2$. Without loss of generality, we can change the scale of z to make $r = 1$. Since the angular momentum is zero, the dynamical variables are only the shape variables. The Lagrangian for $dz = id\tau$ is

$$\mathcal{L} = \mathcal{K} + \mathcal{U}, \quad (120)$$

$$\mathcal{K} = \frac{1}{(1 + \eta\tilde{\eta})^2} \frac{d\eta}{dz} \frac{d\tilde{\eta}}{dz} = \frac{-1}{(1 + \eta\tilde{\eta})^2} \frac{d\eta}{d\tau} \frac{d\tilde{\eta}}{d\tau}, \quad (121)$$

$$\mathcal{U} = \left(\frac{1 + \eta\tilde{\eta}}{2} \right) \left(1 + \frac{4}{(1 - \sqrt{3}\eta)(1 - \sqrt{3}\tilde{\eta})} + \frac{4}{(1 + \sqrt{3}\eta)(1 + \sqrt{3}\tilde{\eta})} \right). \quad (122)$$

The equations of motion are

$$\frac{d^2\tilde{\eta}}{d\tau^2} = \frac{2\eta}{1 + \eta\tilde{\eta}} \left(\frac{d\tilde{\eta}}{d\tau} \right)^2 - (1 + \eta\tilde{\eta})^2 \frac{\partial}{\partial \eta} \mathcal{U}, \quad \text{and } \eta \leftrightarrow \tilde{\eta}. \quad (123)$$

Let $\tau = 0$ be the time of the simultaneous ‘‘half collision’’. Since, we take the path $z = t_{\text{Euler}} + i\tau$, $\tilde{\eta} = -(\eta)^*$ follows. Expanding η and $\tilde{\eta}$ by τ ,

$$\eta = \frac{1}{\sqrt{3}}(1 + a\tau^\lambda), \quad \tilde{\eta} = \frac{-1}{\sqrt{3}}(1 + a^*\tau^{\lambda^*}), \quad \Re\lambda > 0. \quad (124)$$

Substitute this expansion to \mathcal{K} , \mathcal{U} , using $(1 + \eta\tilde{\eta}) \sim 2/3 + \dots$, the main term is

$$\mathcal{K} \sim \frac{-9}{4} \left(\frac{a\lambda}{\sqrt{3}} \tau^{\lambda-1} \right) \left(-\frac{a^*\lambda^*}{\sqrt{3}} \tau^{\lambda^*-1} \right) = \frac{3}{4} aa^* \lambda \lambda^* \tau^{\lambda+\lambda^*-2}, \quad (125)$$

and

$$\mathcal{U} \sim \frac{1}{3} \left(-\frac{2}{a} \tau^{-\lambda} - \frac{2}{a^*} \tau^{-\lambda^*} \right). \quad (126)$$

Therefore, to get $\mathcal{E} = \mathcal{K} - \mathcal{U} = 0$ namely to get $\mathcal{K} \sim \mathcal{U}$ in the main term, $\lambda + \lambda^* - 2 = -\lambda = -\lambda^*$. Namely $\lambda = \lambda^* = 2/3$ and

$$\frac{3}{4} aa^* \times \frac{4}{9} = -\frac{2}{3} \times \frac{a + a^*}{aa^*}. \quad (127)$$

Thus, we have

$$(aa^*)^2 = -2(a + a^*). \quad (128)$$

The equation of motion for η and $\tilde{\eta}$ in the series (124) with $\lambda = \lambda^* = 2/3$ yields

$$-\left(\frac{a^2 a^* + 4}{2\sqrt{3}a^2} \right) \tau^{-4/3} + O(t^{-2/3}) = 0, \quad \left(\frac{a(a^*)^2 + 4}{2\sqrt{3}(a^*)^2} \right) \tau^{-4/3} + O(t^{-2/3}) = 0. \quad (129)$$

Therefore, $a^2 a^* = a(a^*)^2 = -4$. This equation has only one solution $a = a^* = -2^{2/3}$. Since this solution satisfies (127), this solution has zero energy. Thus, the only one solution is given by (119).

A comment: If a and a^* are free parameters $a = a^* = -2^{2/3}\omega$, $\omega^3 = 1$ are solutions.

6.2.1 A simple solution

For the next order,

$$\begin{aligned} \eta(\tau) &= \frac{1}{\sqrt{3}} \left(1 - 2^{2/3} \tau^{2/3} + b \tau^{4/3} \right) + O(t^2), \\ \tilde{\eta}(\tau) &= -\frac{1}{\sqrt{3}} \left(1 - 2^{2/3} \tau^{2/3} + b^* \tau^{4/3} \right) + O(t^2), \end{aligned} \quad (130)$$

the equation of demand only $b = b^*$. The total energy $\mathcal{E} = 0$ demands $b = -3 \times 2^{-2/3}$. Then, for the higher order terms, the equations of motion determine the coefficients,

$$\eta(\tau) = -\tilde{\eta}(\tau) = \frac{1}{\sqrt{3}} \left(1 - 2^{2/3} \tau^{2/3} - \frac{3}{2^{2/3}} \tau^{4/3} - \frac{37}{28} \tau^2 - \frac{5}{56 \times 2^{1/3}} \tau^{8/3} + O(t^{10/3}) \right). \quad (131)$$

Once we assume $\eta = -\tilde{\eta}$, the Lagrangian is simply

$$\begin{aligned} \mathcal{K} &= \frac{+1}{(1 - \eta^2)^2} \left(\frac{d\eta}{d\tau} \right)^2, \\ \mathcal{U} &= \left(\frac{1 - \eta^2}{2} \right) \left(1 + \frac{8}{1 - 3\eta^2} \right). \end{aligned} \quad (132)$$

Then, $\mathcal{E} = \mathcal{K} - \mathcal{U} = 0$ yields

$$\left(\frac{d\eta}{d\tau}\right)^2 = \frac{3(1-\eta^2)^3(3-\eta^2)}{2(1-3\eta^2)}. \quad (133)$$

So, this case is integrable.

Again, I would like to stress that *although this is a solution of the equations of motion for $\alpha = 2$ with total energy zero, constant moment of inertia and vanishing angular momentum, this is not the behavior of the figure-eight solution on the line $z = t_{Euler} + i\tau$.*

Note that the series replacing $\tau^{2/3} \rightarrow \tau^{2/3}\omega$, $\omega^3 = 1$ is also a solution of the equation of motion and the total energy zero. This means that if we forget about the condition $\tilde{\eta} = -(\eta)^*$, and if we put the condition $\eta = -\tilde{\eta}$, the solution is a solution of (133) and the series

$$\eta(\tau) = -\tilde{\eta}(\tau) = \frac{1}{\sqrt{3}} \left(1 - 2^{2/3}\tau^{2/3}\omega - \frac{3}{2^{2/3}}\tau^{4/3}\omega^2 - \frac{37}{28}\tau^2\omega^3 - \frac{5}{56 \times 2^{1/3}}\tau^{8/3}\omega^4 + O(t^{10/3}) \right). \quad (134)$$

is a solution.